Manganese(III) Biliverdin IX Dimethyl Ester: A Powerful Catalytic Scavenger of Superoxide Employing the Mn(III)/Mn(IV) Redox Couple

Ivan Spasojević,[†] Ines Batinić-Haberle,[†] Robert D. Stevens,[‡] Peter Hambright,[§] Arthur N. Thorpe,[#] Jan Grodkowski,[⊥] Pedatsur Neta,[⊥] and Irwin Fridovich*[,†]

Department of Biochemistry and Department of Pediatrics, Duke University Medical Center, Durham, North Carolina 27710, Departments of Chemistry and Physics, Howard University, Washington, D.C. 20059, and Physical and Chemical Properties Division, National Institute of Standards and Technology, Gaithersburg, Maryland 20899-8381

Received May 9, 2000

A manganese(III) complex of biliverdin IX dimethyl ester, $\{Mn^{III}BVDME\}_2$, was prepared and characterized by elemental analysis, UV/vis spectroscopy, cyclic voltammetry, chronocoulometry, electrospray mass spectrometry, freezing-point depression, magnetic susceptibility, and catalytic dismuting of superoxide anion ($O_2^{\bullet-}$). In a dimeric conformation each trivalent manganese is bound to four pyrrolic nitrogens of one biliverdin dimethyl ester molecule and to the enolic oxygen of another molecule. This type of coordination stabilizes the +4 metal oxidation state, whereby the +3/+4 redox cycling of the manganese in aqueous medium was found to be at $E_{1/2} = +0.45$ V vs NHE. This potential allows the Mn(III)/Mn(IV) couple to efficiently catalyze the dismutation of $O_2^{\bullet-}$ with the catalytic rate constant of $k_{cat} = 5.0 \times 10^7\ M^{-1}\ s^{-1}$ (concentration calculated per manganese) obtained by cytochrome *c* assay at pH 7.8 and 25 °C. The fifth coordination site of the manganese is occupied by an enolic oxygen, which precludes binding of $NO^{\bullet}$, thus enhancing the specificity of the metal center toward $O_2^{\bullet-}$. For the same reason the $\{Mn^{III}BVDME\}_2$ is resistant to attack by H_2O_2. The compound also proved to be an efficient SOD mimic in vivo, facilitating the aerobic growth of SOD-deficient *Escherichia coli.*

Introduction

The capacity of natural and synthetic compounds to scavenge oxygen radicals and thus protect tissue from oxidative injury has received increasing attention in recent years.[1,2] Our laboratory has been engaged in the development of metalloporphyrin-based superoxide dismutase (SOD) mimics and scavengers of oxygen reactive species[3−8] that are being pursued as potential pharmaceuticals.[3,9,10] Most of the metalloporphyrins studied thus far were cationic.[2,3,11−15] More hydrophobic compounds are anticipated to be better able to pass biological membranes such as the blood−brain barrier. In pursuing this goal a lipophilic manganese(III) biliverdin dimethyl ester, shown in Scheme 1, whose SOD-like potency is similar to that of the water-soluble cationic Mn(III) tetrakis(*N*-methyl(ethyl)pyridinium-2-yl)porphyrin,[3,4] has been prepared and characterized.

Experimental Section

Materials. General Reagents. The biliverdin IX dimethyl ester (H_3BVDME), bilirubin IX (H_4BR), and bilirubin IX dimethyl ester (H_4BRDME) were obtained from Frontier Scientific (Logan, UT). Biliverdin IX dimethyl ester was further recrystallized from chloroform/petroleum ether at a 15/50 v/v ratio. Petroleum ether (35−60 °C fraction), chloroform, acetone, diethyl ether (anhydrous), 30% solution of H_2O_2, HCl, KCl, KNO_3, EDTA, glucose, phosphate salts, inorganic salts and KOH were from Mallinckrodt, and dichloromethane was from EM Science, and all were of the highest purity. Sodium dithionite (purified) and ammonium oxalate were from J. T. Baker. Manganese-(II) acetate tetrahydrate (99.99%), manganese(II) chloride tetrahydrate (99.99%), sodium L-ascorbate (99+ %), ferrocenemethanol (97%), $K_3Fe(CN)_6$, bromoform (99+%, further redistilled), oxalic acid (99+%), $NaNO_2$ (97+ %), sodium ascorbate (99+%), and methyl-d_3 alcohol-*d* (99.8 atom % D) were from Aldrich, and casamino acids were from

* Author to whom the correspondence should be addressed.
[†] Department of Biochemistry, Duke University Medical Center.
[‡] Department of Pediatrics, Duke University Medical Center.
[§] Department of Chemistry, Howard University.
[#] Department of Physics, Howard University.
[⊥] National Institute of Standards and Technology.

(1) (a) Fridovich, I. *J. Biol. Chem.* **1997**, *272*, 18515. (b) *Oxygen Radicals and the Disease Process*; Thomas, C. E., Kalyanaraman, B., Eds.; Harwood Academic Publishers (HAP): Amsterdam, 1997.
(2) Riley, D. P. *Chem. Rev.* **1999**, *99*, 2573.
(3) Batinić-Haberle, I.; Spasojević, I.; Hambright, P.; Benov, L.; Crumbliss, A. L.; Fridovich, I. *Inorg. Chem.* **1999**, *38*, 4011.
(4) Batinić-Haberle, I.; Benov, L.; Spasojević, I.; Fridovich, I. *J. Biol. Chem.* **1998**, *273*, 24521.
(5) Batinić-Haberle, I.; Liochev, S. I.; Spasojević, I.; Fridovich, I. *Arch. Biochem. Biophys*. **1997**, *343*, 225.
(6) Kachadourian, R.; Batinić-Haberle, I.; Fridovich, I. *Inorg. Chem.* **1999**, *38*, 391.
(7) Day, B. J.; Batinić-Haberle, I.; Crapo, J. D. *Free Radical Biol. Med.* **1999**, *26*, 730.
(8) Ferrer-Sueta, G.; Batinić-Haberle, I.; Spasojević, I.; Fridovich, I.; Radi, R. *Chem. Res. Toxicol*. **1999**, *12*, 442.
(9) Parks, D. A.; Fridovich, I.; O'Donnell, V. B.; Wang, Z.; Batinić-Haberle, I.; Day, B. J.; Chumley, P. H.; Freeman, B. A. *Free Radical Biol. Med*. **1998**, *25 (Suppl. 1)*, S36.
(10) (a) Mackensen, G. B.; Patel, M.; Calvi, C. L.; Batinić-Haberle, I.; Day, B. J.; Fridovich, I.; Crapo, J. D.; Pearlstein, R. D.; Warner, D. S. submitted to J. Neuroscience. (b) Vujašković, Z.; Batinić-Haberle, I.; Spasojević, I.; Anscher, M. S.; Dewhirst, M. W.; Fridovich, I. Unpublished data.
(11) Lee, J.; Hunt, J. A.; Groves, J. T. *J. Am. Chem. Soc.* **1998**, *120*, 6053.
(12) Lee, J.; Hunt, J. A.; Groves, J. T. *J. Am. Chem. Soc.* **1998**, *120*, 7493.
(13) Pasternack, R. F.; Gibbs, E. J.; Villafranca, J. J. *Biochemistry* **1983**, *22*, 5409.
(14) Salvemini, D.; Wang, Z.-Q.; Stern, M. K.; Currie, M. G.; Misko, T. P. *Proc. Natl. Acad. Sci. U.S.A.* **1998**, 95, 2659.
(15) Misko, T. P.; Highkin, M. K.; Veenhuizen, A. M.; Manning, P. T.; Stern, M. K.; Currie, M. G.; Salvemini, D. *J. Biol. Chem.* **1998**, *273*, 15646.

10.1021/ic0004986 CCC: $20.00
Published on Web 01/10/2001

Scheme 1

a) "open" ligand (keto form) - biliverdin IX dimethyl ester, H_3BVDME:

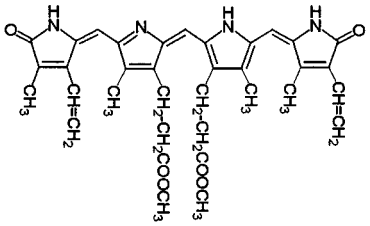

b) "closed" ligand (enol form) - biliverdin IX dimethyl ester, H_3BVDME:

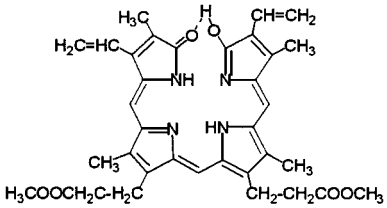

c) dimeric manganese complex, $\{Mn^{III}BVDME\}_2$:

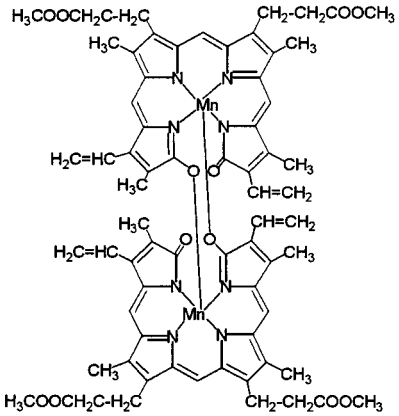

d) MM2 force-field simulation of $\{Mn^{III}BVDME\}_2$:
(peripheral functional groups omitted for clarity)

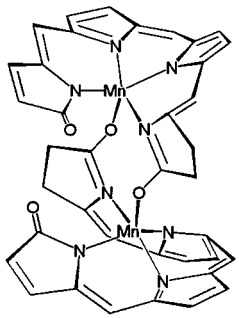

Difco. The volumetric standards, 1.0 and 0.10 M NaOH and lithium hydroxide (anhydrous), were from Fisher Scientific. The 2-methyl-2-propanol (t-BuOH, 99.5+ %), albumin from bovine serum, Pipes disodium salt monohydrate (1,4-piperazinebis(ethanesulfonic acid), succinic acid, *m*-chloroperoxybenzoic acid (85%), and xanthine were purchased from Sigma. Deuterium oxide (D_2O, 99.9%) was from Cambridge Isotope Laboratories. Cytochrome *c* from horse heart (# 30 396), biliverdin IX dihydrochloride ($H_3BV{\cdot}2HCl$) (~80%), 4,4′-bipyridyl (99+%), and *N*,*N*′-bis(salicylidene)ethylenediamine (H_2salen) (99+%) were from Fluka. Xanthine oxidase was prepared by R. D. Wiley and was supplied by K. V. Rajagopalan.[16] Catalase was from Boehringer. Ultrapure argon was from National Welders Supply Co, and nitric oxide was from Matheson Gas Products. Tris (ultrapure) was from ICN Biomedicals, Inc, NONOate NOC-9 was from CalBiochem and phosphate buffered-saline (PBS buffer) from Life Technologies. Gold gauze (52 mesh) was bought from Alfa *A*ESAR. Lithium hydrogen succinate was prepared by neutralizing a 1 M methanolic solution of succinic acid with 0.5 molar equiv of LiOH in methanolic solution. Biliverdin and bilirubin 1 mM aqueous stock solutions (pH ~10) and 0.3 mM methanolic stock solutions of biliverdin dimethyl ester and bilirubin dimethyl ester were used throughout this work. Elemental analyses were made by Atlantic Microlab, Inc. Norcross, GA.

Biliverdin IX Dimethyl Ester. The spectral properties of $BVDME^{3-}$, whose protonated keto and enol forms[17] are shown in Scheme 1a,b, are $\epsilon_{666} = 1.28 \times 10^4\ cm^{-1}\ M^{-1}$ and $\epsilon_{375} = 4.45 \times 10^4\ cm^{-1}\ M^{-1}$, in accordance with literature data.[17] Calcd elemental analysis of H_3BVDME, $C_{35}H_{38}N_4O_6$: C, 68.83; H, 6.27; N, 9.17. Found: C, 68.72; H, 6.25; N, 9.17. The base peak in the electrospray mass spectrum at $m/z = 611$ is assigned to the fully protonated biliverdin dimethyl ester, H_4BVDME^+.

Manganese(III) Porphyrins. Mn^{III}TPPCl and Mn^{III}TSPPNa_3, obtained from Mid-Century Chemicals (Chicago, IL), and Mn^{III}OEPCl, from Aldrich, were used as received. Mn^{III}TM(E)-2(4)-PyPCl_5 and Mn^{II}OBTM-4-PyPCl_4 were prepared as described previously.[3-5]

Manganese(III) Salen. The compound was prepared by the published procedure.[18] Uv/vis in water: $\epsilon_{235} = 3.70 \times 10^4\ cm^{-1}\ M^{-1}$, $\epsilon_{279} = 1.70 \times 10^4\ cm^{-1}\ M^{-1}$, $\epsilon_{397} = 4.60 \times 10^3\ cm^{-1}\ M^{-1}$. Calcd elemental analysis for Mn^{III}salenCl, $C_{16}H_{14}N_2O_2MnCl$: C, 53.88; H, 3.96; N; 7.85. Found: C, 54.02; H, 4.06; N, 7.85. The metal-centered redox potential for the Mn(III)/Mn(II) couple, determined as described previously by cyclic voltammetry,[3] was found to be $E_{1/2} = -0.23$ V vs Ag/AgCl in methanol. On the basis of the $E_{1/2}$ of $Mn^{III/II}$TM-2-$PyP^{5+/4+}$, ferrocene-methanol and of $K_3Fe(CN)_6$ in water and methanol (see under Electrochemistry), the redox potential of Mn^{III}salen$^+$ in water was calculated to be $E_{1/2} = -0.13$ V vs NHE.

Manganese(III) Biliverdin IX Dimethyl Ester, $\{Mn^{III}BVDME\}_2$. The complex was prepared by a modification of literature methods for the synthesis of similar compounds.[19,20] Accordingly, 50 mg of the recrystallized biliverdin dimethyl ester was dissolved in a small volume of chloroform and 150 mL of methanol was added. The mixture was heated to ~60 °C followed by the addition of a 15-fold excess of manganese(II) acetate (0.3 g in 10 mL methanol). The complex formed immediately, as was evident from the disappearance of the absorption at 666 nm and appearance of a band at 898 nm. (Caution: prolonged exposure at ~60 °C results in destruction of the compound.) Most of the solvent was then evaporated on a rotary evaporator at room temperature. Two milliliters of methanol was added for solubilization, followed by 200 mL of chloroform and 200 mL of water. The mixture was poured into a separatory funnel, and the metal complex was extracted into the chloroform layer and washed three times with water. Finally, the chloroform layer was shaken with 5 g of dry $MgSO_4$, followed by filtration and evaporation of the solvent almost to dryness. The residue was transferred to a conical flask and dissolved in 4 mL of dichloromethane. Addition of ~40 mL of petroleum ether gave a precipitate that was collected on a finely fritted glass disk, washed with petroleum ether, and dried overnight in vacuo at room temperature. The yield was >80%. The resultant olive-green compound was soluble in ethanol and methanol but was of very low solubility ($\sim 10^{-8}$ M) in water. The UV/vis characteristics of $\{Mn^{III}BVDME\}_2$, given below are

(16) Waud, W. R.; Brady, F. O.; Wiley: R. D.; Rajagopalan, K. V. *Arch. Biochem. Biophys.* **1975**, *19*, 695.
(17) (a) Gray, C. H.; Lichtarowicz-Kulczycka, A.; Nicholson, D. C.; Petryka, Z. *J. Chem. Soc.* 1961, 2264. (b) Bonnett, R.; McDonagh, A. F. *J. Chem. Soc. Chem. Commun.* **1970**, 238. (c) Nichol, A. W.; Morell, D. B. *Biochim. Biophys. Acta* **1969**, *177*, 599. (d) O'Carra, P.; Colleran, E. *J. Chromatog.* **1970**, *50*, 458. (e) Chae, Q.; Song, P.-S. *J. Am. Chem. Soc.* **1975**, *97*, 4176.
(18) Boucher, L. J. *J. Inorg. Nucl. Chem.* **1974**, *36*, 531.
(19) Fuhrhop, J.-H.; Salek, A.; Subramanian, J.; Mengersen, C.; Besecke, S. *Liebigs Ann. Chem.* **1975**, 1131.
(20) Bonnett, R.; Buckley, D. G.; Hamzetash, D. *J. Chem. Soc., Perkin Trans I*, **1981**, 322.

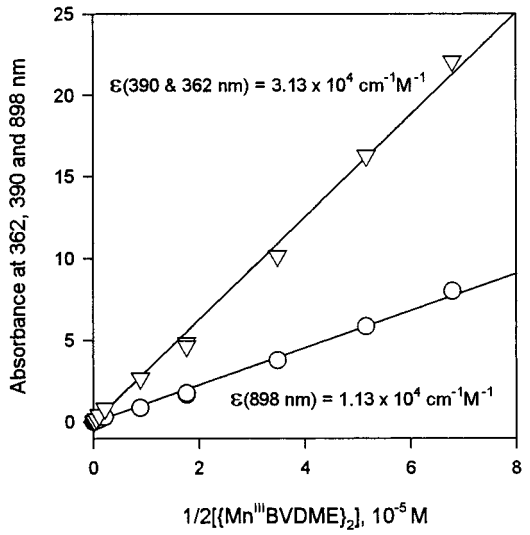

Figure 1. The absorbances at 390, 362, and 898 nm vs 1/2[{Mn^{III}-BVDME}$_2$] in methanol (2×10^{-8} to 8×10^{-5} M). The data were obtained in 1 and 10 cm cells, but are presented as though all were obtained in a 10 cm cell.

in excellent agreement with the literature data for similar compounds.[19] Adherence to the Beer−Lambert law indicates that the same structure exists in methanolic, pyridine, and chloroform solutions in the concentration range from 2×10^{-8} M to 8×10^{-5} M. The molar absorption coefficients are calculated per manganese in methanol (Figure 1), $\epsilon_{898} = 1.13 \times 10^4$ cm^{-1} M^{-1}, $\epsilon_{390} = 3.13 \times 10^4$ cm^{-1} M^{-1}, and $\epsilon_{362} = 3.13 \times 10^4$ cm^{-1} M^{-1}; in pyridine, $\epsilon_{908} = 0.98 \times 10^4$ cm^{-1} M^{-1}, $\epsilon_{393} = 2.80 \times 10^4$ cm^{-1} M^{-1}, and $\epsilon_{367} = 2.80 \times 10^4$ cm^{-1} M^{-1}; and in chloroform, $\epsilon_{898} = 1.07 \times 10^4$ cm^{-1} M^{-1}, $\epsilon_{394} = 2.80 \times 10^4$ cm^{-1} M^{-1}, and $\epsilon_{367} = 2.80 \times 10^4$ cm^{-1} M^{-1}. Calcd elemental analysis for {Mn^{III}BVDME}$_2$, $Mn_2C_{70}H_{70}N_8O_{12}$: C, 63.44; H, 5.33; N, 8.46. Found: C, 62.78; H, 5.41; N, 8.40. The C/N ratio: calcd, 8.74; found, 8.72.

Methods. Electrospray Mass Spectrometry. ESMS measurements were performed on a Micromass-Quattro LC triple-quadrupole mass spectrometer equipped with a pneumatically assisted electrostatic ion source operating at atmospheric pressure. The 600, 60, and 6 μM methanol solutions of $BVDME^{3-}$ and $^1/_2${Mn^{III}BVDME}$_2$ solutions were introduced by loop injection into the methanol stream. The mass spectra were acquired in the continuum mode, scanning from *m*/*z* 600 to 3000 at different cone voltages in the range 30−180 V.

Freezing-Point Depression. The measurements were made in a slowly cooled, rubber-foam-insulated test tube, in which the bulb of a Normalglas precision thermometer (1/100 °C) was completely immersed into 6 mL of the measured solution. Stirring of the solution was accomplished by the slow eccentric movement of the thermometer attached by a flexible connection to a variable-speed motor.

UV/Vis Spectroscopy. The formation and dissociation of {Mn^{III}-BVDME}$_2$ as well as the pH* titration of the ligand, all in methanol/aqueous (9/1, v/v) solutions, were studied at 25 °C on UV-2501PC Shimadzu spectrophotometer. The effects of EDTA, H_2O_2, reductants, and oxidants and the methanol/water ratio on the stability of the Mn(III) complex were also examined, all at 25 °C. The reactivity of {Mn^{III}BVDME}$_2$ toward nitric oxide was determined for the reaction with gaseous NO$^\bullet$ and with the NONOate NOC-9 in a methanol/PBS (1/1, v/v) solution, as described previously.[21] Tris and Pipes buffers along with a 1.0 M methanol/aqueous (9/1) solution of HCl were used for pH* (see Abbreviations) adjustments in methanol/aqueous solutions. The pH* readings were measured on an Oakton pH-Meter equipped with a Denver Instruments combination glass electrode that was calibrated in methanol/water (9/1, v/v) buffer solutions: 10 mM oxalic acid/10 mM ammonium oxalate (pH* = 3.59) and 10 mM succinic acid/lithium hydrogen succinate (pH* = 6.55).[22]

Reduction of {Mn^{III}BVDME}$_2$ was accomplished with ascorbic acid and sodium dithionite, while oxidation was performed with *m*-chloroperoxybenzoic acid in the presence and absence of $NaNO_2$. Reduction and oxidation of {Mn^{III}BVDME}$_2$ were also done by radiolytic methods. Reduction was carried out by irradiation in deoxygenated aqueous methanol solutions as described before for metalloporphyrins.[23] Oxidation was performed with the trichloromethylperoxyl radical by irradiation of air-saturated methanol solutions containing 1% CCl_4 as described before.[24] The radiolysis was performed in a Gammacell 220 ^{60}Co source with a dose rate of 1.3 Gy s^{-1}.

The water-soluble analogue, manganese(III) biliverdin, {$Mn^{III}BV^{2-}$}$_2$, was prepared in water at a 1:1 metal-to-ligand ratio. A pH of at least 10 was required for rapid complexation, possibly via the reactive $MnOH^+$ ion.[25] The complex was prepared at a 1.0 mM (per Mn) level and diluted into 0.05 M phosphate buffer, pH 7.8, as needed. For comparison, biliverdin, bilirubin, and their dimethyl esters were also studied.

Magnetic Susceptibility in Solution. Magnetic susceptibilities were determined by the Evans method[26] at 25 °C using a 400 MHz Varian NMR spectrometer. Typically ∼2 mg of the compound, dissolved in 0.4 mL D_2O or CD_3OD containing 0.01 M t-BuOH, was placed in a NMR tube along with a capillary that contained the same solvent mixture.

Magnetic Susceptibility in the Solid State. Magnetic susceptibility of the solid {Mn^{III}BVDME}$_2$ was measured on a Faraday balance[27−30] automated to record apparent mass changes at programmed temperature and magnetic field intervals. The 5 mg samples were suspended on a Cahn electrobalance with He gas as the heat transfer medium.

Electrochemistry of the Manganese(III) Biliverdin Dimethyl Ester. Measurements were made using a CH Instruments model 600 voltammetric analyzer, as described previously.[3] A three-electrode system in a small volume (0.5−3.0 mL) was used, with a 3 mm diameter glassy carbon button working electrode (Bioanalytical Systems), Ag/AgCl reference electrode (3 M NaCl, Bioanalytical Systems), and a Pt wire (0.5 mm) as auxiliary electrode. Cyclic votammetry was performed on 0.5 mM (per manganese) methanol/aqueous (9/1, v/v) solutions of the compounds investigated. The ionic strength was kept at 0.10 M (NaCl), and 0.05 M Tris buffer was used for pH* adjustment. For calibration purposes compounds of different hydrophilicities, $K_3Fe(CN)_6$,[31] ferrocenemethanol, and Mn^{III}TM-2-PyP^{5+}, were studied in both aqueous and methanol/aqueous (9/1, v/v) solutions (I = 0.10 M NaCl, 0.05 M Tris buffer, pH* 7.9). In all cases the measured $E_{1/2}$ was 170 mV more positive in methanol than in water, and this value was used to predict the redox potential in aqueous solution from measurement in methanol/water. Cyclic voltammetry of a 1 mM (per manganese) solution of {$Mn^{III}BV^{2-}$}$_2$ in 0.05 M phosphate buffer, pH 7.8, 0.1 M NaCl was also performed. Often, Mn^{III}TM-2-PyP^{5+} was added as an internal standard when cyclic voltammetry of {Mn^{III}-BVDME}$_2$ in methanol and of {$Mn^{III}BV^{2-}$}$_2$ in water was performed.

The chronocoulometry measurements were done by recording the change in charge vs time at a fixed potential that was applied to a glassy-carbon button working electrode immersed in 1mM methanol/aqueous (9/1, v/v) solutions (0.1 M NaCl, 0.05 M Tris buffer, pH* 7.9) of $^1/_2${Mn^{III}BVDME}$_2$ and Mn^{III}TM-2-PyP^{5+}.

Thin-layer spectroelectrochemical measurements were done using a 52 mesh gold gauze working electrode. Ag/AgCl was the reference electrode and 0.5-mm platinum wire the auxiliary electrode. Optical

(21) Spasojević, I.; Batinić-Haberle, I.; Fridovich, I. *Nitric Oxide: Biol. Chem.* **2000**, *4*, 526.
(22) De Ligny, C. L.; Luykx, P. F. M.; Rehbach, R.; Wieneke, A. A. *Rec. Trav. Chim. Pays-Bas* **1960**, *79*, 699.
(23) Baral, S.; Hambright, P.; Neta, P. *J. Phys. Chem.* **1984**, *88*, 1595.
(24) Brault, D.; Neta, P. *J. Phys. Chem.* **1984**, *88*, 2857.
(25) Baes, C. F.; Mesmer, R. E. *The Hydrolysis of Cations;* Wiley & Sons: New York 1976.
(26) Evans, D. F. *J. Chem. Soc.* **1959**, 2003.
(27) Hambright, P. *Chemistry of Water-Soluble Porphyrins*, In *The Porphyrin Handbook*; Kadish, K. M., Smith, K. M., Guillard, R., Eds.; Academic Press: New York, 2000; Chapter 18.
(28) Thorpe, A. N.; Senftle, F. E. *Rev. Sci. Inst.* **1959**, *30*, 1006.
(29) Sullivan, S.; Thorpe, A. N.; Hambright, P. *J. Chem. Educ.* **1971**, *48*, 345.
(30) Thorpe, A. N.; Senftle, F.; Finkleman, F.; Dulong, F.; Bostick, N. *Coal Geol.* **1998**, 36, 243.
(31) Kolthof, I. M.; Tomsicek, W. J. *J. Phys. Chem.* **1935**, *39*, 945.

spectra were taken on a UV-2501PC Shimadzu spectrophotometer.

Catalysis of $O_2^{\bullet-}$ Dismutation: Cytochrome *c* Assay. Catalysis of the dismutation of $O_2^{\bullet-}$ in vitro was followed by the xanthine oxidase/cytochrome *c* method.[32] The xanthine/xanthine oxidase reaction was the source of $O_2^{\bullet-}$, and ferricytochrome *c* was used as the indicating scavenger of $O_2^{\bullet-}$. The reduction of cytochrome *c* was followed at 550 nm, and the assays were conducted in 0.05 M phosphate buffer, pH 7.8, in the presence and absence of albumin and 15 μg/mL catalase. $O_2^{\bullet-}$ was produced at a rate of 1.2 μM/min. The concentration of EDTA was varied between 10^{-4} M and 10^{-2} M in order to ensure that the effects observed were not due to the presence of free metal ions. The EDTA complexes of Mn(II),[33] Fe(II),[34] and Cu(II)[35] were previously found to be SOD-inactive. All measurements were at 25 °C.

Pulse Radiolysis. Pulse radiolysis experiments were carried out with a Varian[36] linear accelerator, which provides 0.05−1.5 μs pulses of 6 MeV electrons, producing up to 30 μM radicals in irradiated solutions at (22 ± 1) °C. The kinetic spectrophotometric detection system utilized a Hamamatsu 75 W xenon lamp, a shutter and optical cutoff filters to minimize photolysis of the solution, a 2 cm optical path length irradiation cell, a Jobin-Yvon monochromator, a Hamamatsu R955 photomultiplier, and a Tektronix 420A digitizing oscilloscope. Due to the water-insolubility of $\{Mn^{III}BVDME\}_2$ at the micromolar concentration levels, a study of 1/1 and 1/4 methanol/0.05 M phosphate buffer (pH 7.8) solutions was attempted, with a limited success. Thus the data obtained in a mixed methanol/water system showed significant impact of the methanol and could not be readily compared to the data obtained by cytochrome *c* assay in an all-aqueous medium. Pulse radiolysis required micromolar levels, while the cytochrome *c* assay allows working at nanomolar levels of $\{Mn^{III}BVDME\}_2$. To overcome such difficulties we used both methods to determine the catalytic rate constant for the dismutation of $O_2^{\bullet-}$ by the water-soluble analogue $\{Mn^{III}BV^{2-}\}_2$ in an all-aqueous medium (0.05 M phosphate buffer, pH 7.8).

Effects on *Escherichia coli*. *E. coli* strains AB1157 (SOD-proficient, wild type) and JI132 (SOD-deficient, sodAsodB) were kindly supplied by J. A. Imlay.[37] The effect of $BVDME^{3-}$ and $\{Mn^{III}BVDME\}_2$ on the growth of these strains was followed aerobically in minimal (five amino acids) medium at 37 °C.[38] Cultures were treated as previously described.[38,39] Due to the low water solubility, the compounds were solubilized with albumin in the medium at a 1:1 molar ratio, and albumin itself had no effect on growth in the concentration range employed. Since methanol (but not ethanol) was toxic to the SOD-deficient strain of *E. coli* when present in the medium at 0.15%, the stock solutions of the compounds were prepared in ethanol.

Results

Electrospray Mass Spectrometry. The dimeric manganese(III) biliverdin dimethyl ester (Scheme 1) is neutral and can only be observed in ESMS by association with cations, presumably at enolic oxygens or by metal-centered electrochemical oxidation at the capillary tip.[40] By comparison to $(H_2O)Mn^{III}P$ and $HOFe^{III}P$ (P = *N*-alkylpyridylporphyrins), which are easily reduced at the metal centers,[3,41] the manganese(III) biliverdin dimethyl ester is not readily reduced to the Mn(II) state but is more easily oxidized to Mn(IV) (see under Electrochemistry). Consequently, the mass spectra of the metalloporphyrins contain peaks of reduced species whose intensities depend on the applied cone voltage.

Examples of the ESMS spectra are given in Figure 2a and the peak assignments in Table 1. In Figure 2b the intensities of the major ions are given as a function of cone voltage. The isotopic distribution was accounted for in the calculation of ion intensities. At a low cone voltage (30 V) the spectrum shows two major peak groups of similar relative intensities, one around *m*/*z* 1325 and the other region around *m*/*z* 662. We assign the dominant peak at *m*/*z* 1325 to the protonated dimeric structure $\{Mn^{III}BVDME, Mn^{III}HBVDME^+\}$, and the peak at *m*/*z* 1324 to the species oxidized at the metal site, $\{Mn^{IV}BVDME^+, Mn^{III}BVDME\}$. The higher the cone voltage, the lower the intensities of these peaks relative to those ions at *m*/*z* 662 and 663 (Figure 2b). The latter ions are observed as a consequence of the collision-induced dissociation of the oxidized and protonated dimer, respectively (Table 1). As the cone voltage increases from 30 to 150 V, the relative intensities of the cationic species that bear H^+, Na^+, or K^+ increases. Moreover, the higher the cone voltage, the higher the ratio of sodiated over protonated species, reflecting the relative stability of the cationic species. In addition, the ratio of oxidized to cationic dimer decreases, and thus, the ratio of oxidized to cationic monomer increases. The persistence of the dimer at cone voltages as high as 180 V is indicative of its high stability. At cone voltages approaching 180 V, more of the ligand becomes detectable at *m*/*z* 611. The peaks at *m*/*z* 1987 and 1988 may be assigned either to the oxidized and protonated (monomer + dimer) cluster or to the oxidized or protonated trimer, respectively.

When a methanolic solution of $\{Mn^{III}BVDME\}_2$ was diluted 10- and 100-fold, the degree of fragmentation was increased in the same manner as when the cone voltage was elevated. Dilution also increased the ratio of Na^+ and K^+ to H^+, thus increasing the intensities of sodiated and potassiated species. At a 100-fold dilution, the relative intensity of the dimeric species is still high. Thus, ∼20% of the oxidized and ∼20% of the sodiated ion were seen at a cone voltage of 60 V.

In an attempt to further understand the processes underlying the changes in the mass spectrum with cone voltage, selected ions were fragmented in the collision cell. The parent ion *m*/*z* 1324 gave *m*/*z* 662 as the only product ion, whereas *m*/*z* 1325 gave both *m*/*z* 662 and 663. The latter is readily explained, since the peak at *m*/*z* 1325 is due both to the protonated dimer and to the heavy ^{13}C isotope of the oxidized dimer. Similar experiments with trimeric species gave dimeric and monomeric ions.

Several ions were observed only at the lowest threshold (30 V) cone voltage, e.g. *m*/*z* 674, 693, and 1005. Interestingly, the isotope distribution for these ions was *m*/*z* 0.5, indicating that they were doubly charged. Therefore, the *m*/*z* 674 is either a cluster of protonated and sodiated monomers or a doubly charged dimer. In either case it is easily collisionally dissociated. Similarly, the doubly charged *m*/*z* 1005 is either a cluster of monomer and dimer or trimer. Most of the ions observed at the threshold cone voltage may be explained (Table 1) on the basis of singly and multiply charged ions. The origin of the persistent signal at 717 is not known.

Finally, we compared the ESMS behavior of $Mn^{III}OEPCl$, which should have a lipophilicity similar to $\{Mn^{III}BVDME\}_2$. The base peak was the $Mn^{III}OEP^+$ ion at *m*/*z* 587, and less than 2% of a dimer was observed at the lowest cone voltage (30 V) for a concentrated (2 mM) solution. This is in marked contrast

(32) McCord, J. M.; Fridovich, I. *J. Biol. Chem.* **1969**, *244*, 6049.
(33) Archibald, F. S.; Fridovich, I. *J. Bacteriol.* **1981**, *145*, 442.
(34) DiGuiseppi, J.; Fridovich, I. *Arch. Biochem. Biophys.* **1980**, *203*, 145.
(35) Koppenol, W. H.; Van Buuren, K. J. H.; Butler, J., Braams, R. *Biochim. Biophys. Acta* **1976**, *449*, 157.
(36) The mention of the commercial equipment or material does not imply recognition or endorsement by the National Institute of Standards and Technology, nor does it imply that the material or equipment identified are necessarily the best available for purposes.
(37) Imlay, J. A.; Linn, S. *J. Bacteriol.* **1987**, *169*, 2967.
(38) Faulkner, K. M.; Liochev, S. I.; Fridovich, I. *J. Biol. Chem.* **1994**, *269*, 23471.
(39) Benov, L.; Fridovich, I. *J. Biol. Chem.* **1998**, *273*, 10313.
(40) Van Berkel, G. J. In *Electrospray Ionization Mass Spectrometry, Fundamentals, Instrumentation, And Applications*; Cole, B. R., Ed; Wiley: New York, 1997; p. 65.
(41) Batinić-Haberle, I.; Stevens, D. R.; Fridovich, I. *J. Porphyrins Phthalocyanines* **2000**, *4*, 217.

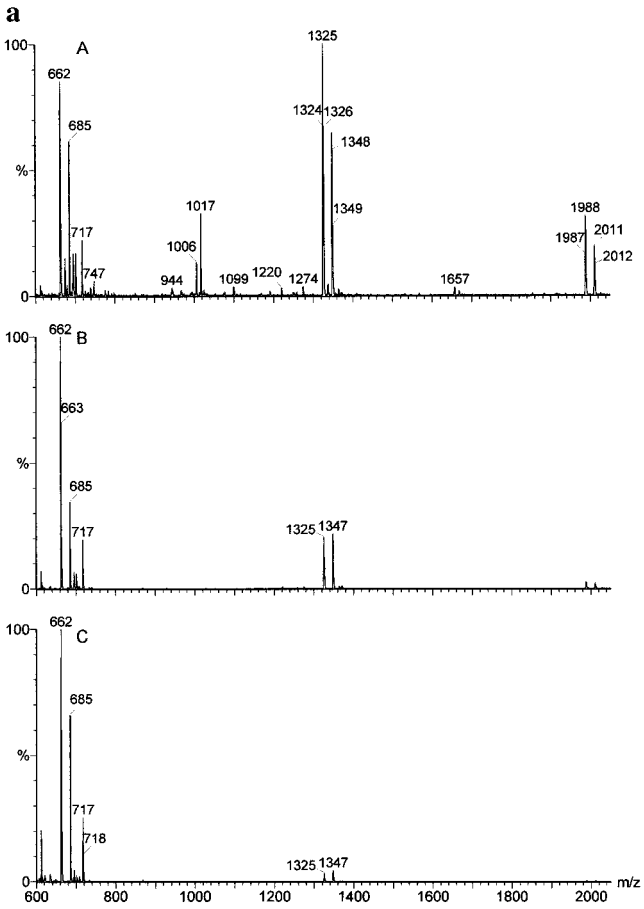

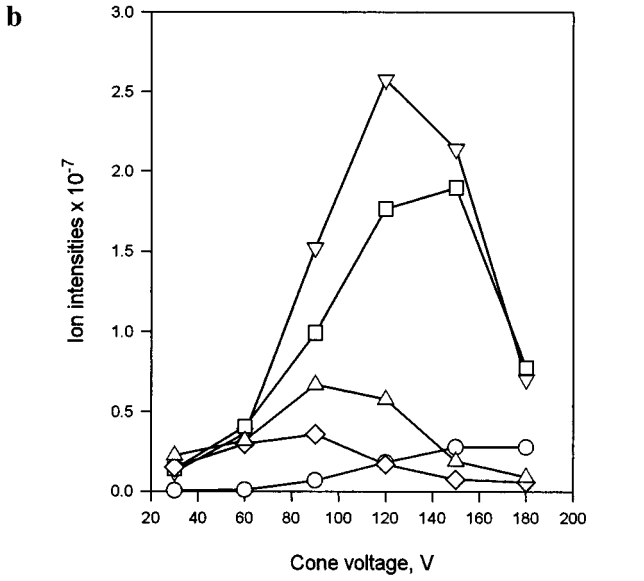

Figure 2. (a) Electrospray mass spectrometry of 600 μM 1/2{Mn^{III}BVDME}$_2$ in methanol at cone voltages of 30 V (A), 90 V (B), and 150 V (C). The ion at *m/z* 1006 is a multiplet for the doubly charged ion, ({Mn^{III}BVDME,Mn^{III}HBVDME$^+$}+Mn^{III}NaBVDME$^+$)$^{2+}$, with ions at *m/z* 1005.4, 1005.9, 1006.4, and 1006.9. (b) The ion intensities of the major peaks as a function of cone voltage: circles, protonated ligand H_4BVDME$^+$; diamonds, oxidized dimer {Mn^{IV}BVDME$^+$,-Mn^{III}BVDME}; triangles up, cationic dimer {Mn^{III}BVDME,-Mn^{III}XBVDME$^+$}, including species that have X as H^+, Na^+, and K^+; squares, cationic monomer, Mn^{III}HBVDME$^+$; triangles down, oxidized monomer, Mn^{IV}BVDME$^+$.

to {Mn^{III}BVDME}$_2$, where dimers persist at all cone voltages and dilutions studied.

Table 1. Electrospray Mass Spectrometry Results of 0.6 mM (per Mn) Methanolic Solutions of Mn(III) Biliverdin Dimethyl Ester

m/z[a]	species
609	H_2BVDME$^+$
611	H_4BVDME$^+$
662[b]	Mn^{IV}BVDME$^+$
663[c]	Mn^{III}HBVDME$^+$
674	(Mn^{III}HBVDME$^+$ + Mn^{III}NaBVDME$^+$)$^{2+}$
685[d]	Mn^{III}NaBVDME$^+$
693	(Mn^{III}NaBVDME$^+$ + Mn^{III}KBVDME$^+$)$^{2+}$
695	Mn^{III}HBVDME$^+$ + CH_3OH
701	Mn^{III}KBVDME$^+$
994	({Mn^{III}BVDME,Mn^{III}HBVDME$^+$}+Mn^{III}HBVDME$^+$)$^{2+}$ [e]
1005	({Mn^{III}BVDME,Mn^{III}HBVDME$^+$}+Mn^{III}NaBVDME$^+$)$^{2+}$ [e]
1017	({Mn^{III}BVDME,Mn^{III}NaBVDME$^+$}+Mn^{III}NaBVDME$^+$)$^{2+}$ [e]
1274	(H_4BVDME$^+$+Mn^{II}HBVDME)$^+$
1324	{Mn^{IV}BVDME$^+$,Mn^{III}BVDME}
1325	{Mn^{III}BVDME,Mn^{III}HBVDME$^+$}
1347	{Mn^{III}BVDME,Mn^{III}NaBVDME$^+$}
1987	({Mn^{IV}BVDME$^+$,Mn^{III}BVDME}+Mn^{III}BVDME)$^+$ [f]
1988	({Mn^{III}BVDME,Mn^{III}HBVDME$^+$}+Mn^{III}HBVDME)$^+$ [f]
2010	({Mn^{III}BVDME,Mn^{III}NaBVDME$^+$}+Mn^{III}BV DME)$^+$ [f]

[a] The peaks listed were obtained in the range of cone voltages from 30 to 180 V. The peaks that correspond to the isotopic pattern are not given. [b] Doubly oxidized. [c] Doubly protonated. [d] Doubly sodiated dimers are buried under these signals. [e] The peaks at *m/z* 1987, 1988, and *m/z* 2010 could as well be assigned to singly charged oxidized {Mn^{IV}BVDME$^+$,Mn^{III}BVDME,Mn^{III}BVDME}, protonated {Mn^{III}BVDME,Mn^{III}BVDME,Mn^{III}HBVDME$^+$}, and sodiated trimer Mn^{III}BVDME,Mn^{III}BVDME,Mn^{III}NaBVDME$^+$}, respectively. [f] Also, the peaks at *m/z* 994, 1005 and, 1017 may be assigned to doubly charged protonated {Mn^{III}HBVDME$^+$,Mn^{III}BVDME,Mn^{III}HBVDME$^+$}, mixed protonated and sodiated {Mn^{III}HBVDME$^+$,Mn^{III}BVDME,-Mn^{III}NaBVDME$^+$}, and sodiated trimer {Mn^{III}NaBVDME$^+$,Mn^{III}-BVDME,Mn^{III}NaBVDME$^+$}, respectively (see also under Figure 2a caption).

Freezing-Point Depression. The measurements were made in bromoform on 17 mM solutions of 4,4′-bipyridyl, used as a monomeric standard, and {Mn^{III}BVDME}$_2$ (concentration calculated per manganese). Bromoform was chosen due to its large freezing point depression constant[42] of 14.4 °C m^{-1} and it is a good solvent for both compounds. Three independent measurements on each compound were made, and the data are shown in Figure 3. Exactly twice the freezing-point depression was observed for the monomeric 4,4′-bipyridyl than for equimolar Mn(III) biliverdin dimethyl ester (per manganese concentration), a clear indication of the dimeric state of the latter compound.

UV/Vis Spectroscopy: Manganese Incorporation. At pH* 7.4 biliverdin dimethyl ester is in the fully deprotonated form, BVDME^{3-}. Our data (Figure 4, inset) show that protonation of the BVDME^{3-} occurs at pH* < 4, which is in agreement with previous results on biliverdin.[43] The carboxyl groups are separated from the main chromophores by two methylenes, and their ionizations are not detectable spectrophotometrically. Thus the spectra of biliverdin and its ester are the same.[43] Manganese was readily incorporated into this ligand by using manganese(II) chloride or acetate. At a 1:1 metal-to-ligand ratio (20 μM) the formation of the dimeric complex {Mn^{III}BVDME}$_2$ at pH* 7.4 (methanol/aqueous, 9/1, v/v) goes to completion within 40 min. The multiple isosbestic points (Figure 4) observed during complex formation indicate only two light-absorbing species in equilibrium, which we ascribe to the fully deprotonated ligand

(42) (a) *Handbook of Chemistry and Physics*, 74th ed.; D. R., Lide, Ed.; CRC Press: Boca Raton, 1993−1994. (b) *Lange's Handbook of Chemistry*, 10th ed.; McGraw-Hill: New York, 1966.
(43) (a) Gray, C. H.; Kulczycka, A.; Nicholson, D. C. *J. Chem. Soc.* 1961, 2276. (b) Kuenzle, C. C.; Pelloni, R. R.; Weibel, M. H. *Biochem. J.* **1972**, *130*, 1147. (c) O Carra, P. *Nature* **1962**, 899.

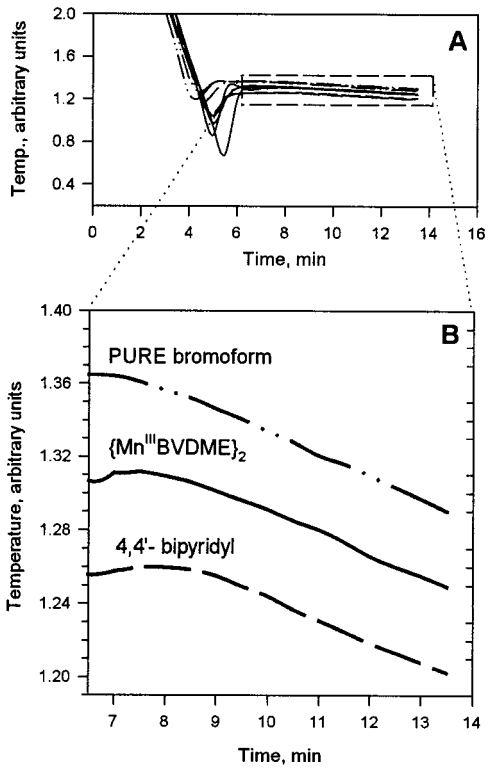

Figure 3. Freezing point measurements of pure bromoform and 16.8 mM (per Mn) Mn(III) biliverdin dimethyl ester and 17.3 mM 4,4′-bipyridyl in bromoform. Three independent measurements were performed (A), and are averaged for clarity in the shorter period of time (B).

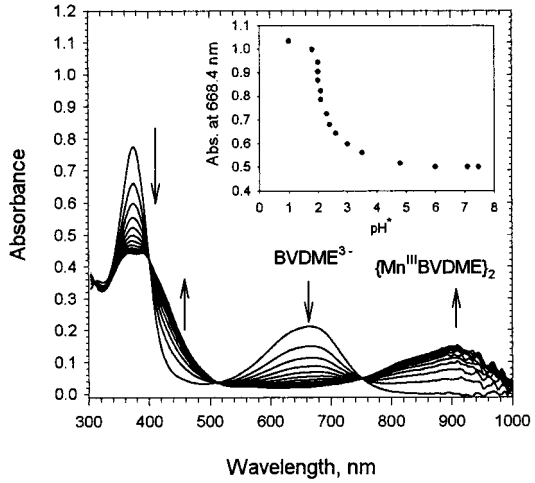

Figure 4. The formation of the $\{Mn^{III}BVDME\}_2$ at 25 °C at 1:1 metal-to-ligand ratio (20 μM $MnCl_2$ and 20 μM $BVDME^{3-}$) in 9/1 (v/v) methanol/aqueous solution, pH* 7.4, 0.05 M Tris buffer. Inset: The absorbance of biliverdin dimethyl ester at 668.4 nm vs pH*, 9/1 methanol/aqeous solution, 0.01 M Tris and Pipes buffer.

and the dimeric metal complex. The kinetic traces recorded upon fast mixing of 30 μM $BVDME^{3-}$ with 75 or 150 μM $MnCl_2$ fit a single-exponential equation. This suggests that the rate-limiting step is the formation of the monomeric complex, followed by fast dimerization to yield $\{Mn^{III}BVDME\}_2$. The monomeric species was not observable spectrophotometrically. Upon decreasing the pH*, the complex dissociates. Six isosbestic points were observed only in the pH* region 7.9−4.5, where the fully deprotonated ligand is the major species. The spectra obtained resemble the spectra shown in Figure 4, where complex formation was followed at pH* 7.4. The isosbestic points become obscure at lower pH as a result of multiple ligand protonations.

Table 2. Second-Order Rate Constants for the Degradation of Mn(III) Biliverdin Dimethyl Ester, Biliverdin, Bilirubin, and Isomeric $Mn^{III}TM(E)$-*X*-PyP^{5+} with H_2O_2 at 25 °C (X = 2, 3, 4)

compound	$k(H_2O_2)$, M^{-1} s^{-1}
H_2TM-2-PyP^{4+} [a]	5×10^{-6}
$Mn^{III}TE$-2-PyP^{5+} [a]	1.3
$Mn^{III}TM$-2-PyP^{5+} [a]	1.3
$Mn^{III}TM$-3-PyP^{5+} [a]	4.9
$Mn^{III}TM$-4-PyP^{5+} [a]	4.6
$\{Mn^{III}BVDME\}_2$ [b]	6.2×10^{-4}
biliverdin [c]	3.0×10^{-3}
bilirubin [c]	1.5×10^{-4}

[a] pH 7.8, 0.05 M phosphate buffer; data from ref 3. [b] pH* 7.9, 9/1 methanol/aqueous solution, 0.05 M Tris buffer, concentration calculated per Mn. [c] 0.05 M Tris buffer, pH 7.8.

Biliverdin (BV^{5-}), similar to its dimethyl ester, reacted with Mn(II) in 9/1 methanol/aqueous solution, pH* 7.9 (Tris buffer), and in water (Tris or phosphate buffer, pH ≥ 10) to form a similar dimeric complex, $\{Mn^{III}BV^{2-}\}_2$. This complex, however, was less stable than its dimethyl ester and did not permit isolation or extensive characterization. Within 30 min only 5% dissociation of $\{Mn^{III}BV^{2-}\}_2$ was observed, thus allowing electrochemical characterization and determination of the rate constant for the catalysis of $O_2^{\bullet-}$ dismutation. The electrostatic repulsions of the negatively charged carboxylates may contribute to the instability of $\{Mn^{III}BV^{2-}\}_2$. The fact that the same UV/vis spectra were observed for the carboxylate and the ester allows us to use the same molar absorption coefficients for concentration calculations.

A very slow hydrolysis of $\{Mn^{III}BVDME\}_2$ occurs in 9/1 methanol/aqueous solution, pH* 7.9. In 1 week at 25 °C only 14% of the complex dissociated. When the water content was increased to 43%, half the complex dissociated in 1 week. A 1 μM 1/2$\{Mn^{III}BVDME\}_2$ solution was stable in the presence of a 900-fold excess of EDTA (0.9 mM) for 24 h in methanol/aqueous (9/1, v/v) solution, 0.05 M Tris, pH* 7.9.

Interaction with H_2O_2. At micromolar concentrations, certain Mn(III) and Fe(III) porphyrins are degraded by H_2O_2 in aqueous solution, pH 7.8.[3,44] However, $\{Mn^{III}BVDME\}_2$ was extremely resistant to H_2O_2. The reaction was followed in 9/1, v/v methanol/aqueous solution at pH* 7.9, 25 °C. In the presence of excess H_2O_2 (6−120 mM) over $\{Mn^{III}BVDME\}_2$ (15 and 30 μM), a second-order rate constant ($k = 6.2 \times 10^{-4}$ M^{-1} s^{-1}) was determined from the linear plot of the observed pseudo-first-order rate constant, k_{obs}, vs $[H_2O_2]$, where $k_{obs} = k[H_2O_2]$. UV/vis spectroscopy indicated degradation via reduction of biliverdin to bilirubin, followed by loss of the metal ion.[43] The interaction of biliverdin and bilirubin with H_2O_2 was also followed in 0.05 M Tris buffer, pH 7.8. As observed for its metal complex, biliverdin undergoes reduction by H_2O_2 to bilirubin. Under pseudo-first-order conditions (6−60 mM H_2O_2, 60 μM biliverdin), k was found to be 3.0×10^{-3} M^{-1} s^{-1}. Bilirubin is more resistant to H_2O_2 than biliverdin or its metal complex. The disappearance of bilirubin was followed at 435 nm[45] under the same conditions with $k = 1.5 \times 10^{-4}$ M^{-1} s^{-1}. The rate constants are given in Table 2 along with those of the cationic *N*-alkylpyridylmetalloporphyrins. Both $BVDME^{3-}$ ligand and its Mn(III) complex are several orders of magnitude more stable in the presence of H_2O_2 than the isomeric Mn(III)

(44) Everett, A. J.; Minkoff, G. *J. Trans. Faraday Soc.* **1953**, *49*, 410.
(45) Gray, C. H.; Kulczycka, A.; Nicholson, D. C. *J. Chem. Soc.* **1961**, 2268.

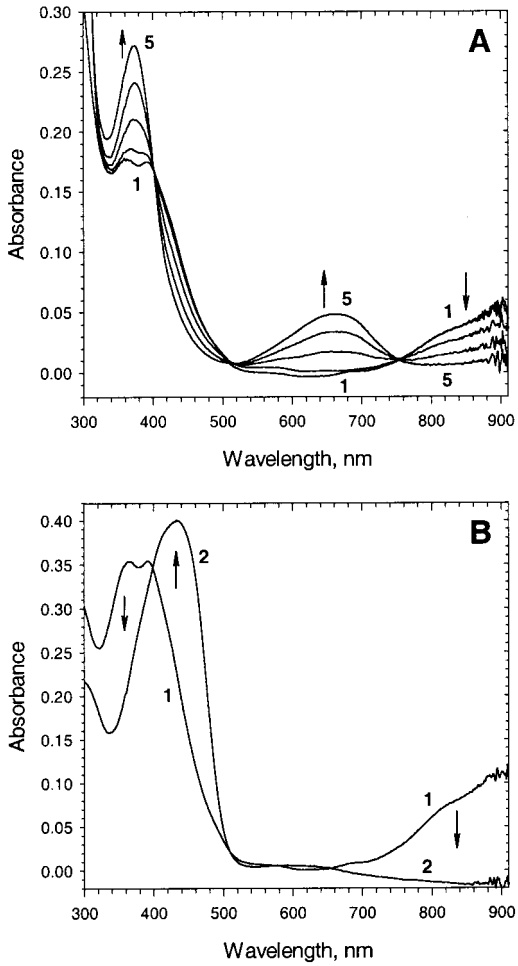

Figure 5. The reduction of 6 μM 1/2{Mn^{III}BVDME}$_2$ with 0.6 mM ascorbic acid in 9/1 (v/v) methanol/aqueous solution, pH* 7.9 (A). The reduction of 12 μM 1/2{Mn^{III}BVDME}$_2$ with 9 mM sodium dithionite in 9/1 (v/v) methanol/aqueous solution, pH* 7.9 (B). In both parts the spectrum 1 was taken in the absence of reductants.

N-alkypyridylporphyrins. Under the conditions given above and at 60 mM H_2O_2, ~40% of the biliverdin and ~14% of bilirubin were degraded within 4.4 h, while ~14% of the complex was degraded within 80 min.

Interaction with NO$^{\bullet}$. No change in the spectrum of 14 μM {Mn^{III}BVDME}$_2$ in the presence of a 90-fold excess NO$^{\bullet}$ in 9/1 methanol/PBS was observed after 1 h.

Reaction with Reductants. (a) Ascorbic Acid. {Mn^{III}-BVDME}$_2$ was not reduced by ascorbate at a 1:1 and 10:1 ascorbate-to-complex ratios ([{Mn^{III}BVDME}$_2$]$_{tot}$ = 3 μM) in 9/1 (v/v) methanol/aqueous solution at pH* 7.9 or in 1/1 (v/v) methanol/0.05 M Tris buffer (pH 7.8) in 24 h. Significant reduction occurred only at 100:1 ascorbate to {Mn^{III}BVDME}$_2$,- and this was followed by demetalation. The spectra exhibit multiple isosbestic points, indicating an equilibrium between the fully deprotonated biliverdin and its manganese complex (Figure 5A). The UV/vis spectra obtained are identical to those given in Figure 4. Similar to {Mn^{III}BVDME}$_2$ ($E_{1/2}$ = −0.23 V vs. NHE, see Table 4 below), Mn^{III}TCPP^{3-} ($E_{1/2}$ = −0.194 V)[3] could not be reduced by ascorbic acid.[46] However, Mn^{III}-TM(E)-2-PyP^{5+} ($E_{1/2}$ = +0.220[3] (0.228)[3] V) and MnTM(E)-4-PyP^{5+} ($E_{1/2}$ = +0.060[3] (0.075)[21] V) are reduced by ascorbate. The metal-free biliverdin dimethyl ester is reduced with ascorbate only at [ascorbate]/[BVDME] > 1000 and even then the reduction takes place over 24 h, with spectral changes indicating reduction of biliverdin to bilirubin. At the same ascorbate to bilirubin dimethyl ester ratio no significant changes in the UV/vis data were observed within 24 h in 9/1 (v/v) methanol/aqueous solution, pH* 7.9.

Table 3. Magnetic Moments for Various Metalloporphyrins, Mn^{III}salen$^+$, {Mn^{III}OEB}$_2$, and {Mn^{III}BVDME}$_2$ in D_2O and CD_3OD Solutions at 25 °C[a]

	magnetic moment, μ_{eff} (μ_B)				
compound	CD_3OD	$CDCl_3$ solid state		D_2O	$\mu_{eff}(D_2O) - \mu_{eff}(CD_3OD)$
Mn^{III}salen$^+$	4.92		4.96[b]	5.35	0.43
Mn^{III}TSPP^{3-}	4.14			4.83, 4.9*c*	0.69
Mn^{III}TE-2-PyP^{5+}	4.00			4.62	0.62
Mn^{III}TM-2(4)-PyP^{5+}	4.14(4.10)			4.57(4.60)	0.43(0.50)
Mn^{III}TPP$^+$	4.10				
{Mn^{III}OEB}$_2$		4.7[d]			
{Mn^{III}BVDME}$_2$	4.57	5.15[e]	4.45	5.10[f]	0.53[g]
Mn^{II}OBTM-4-PyP^{4+}	5.10				

[a] Theoretical spin-only magnetic moments for Mn(III) and Mn(II) high-spin complexes with four and five unpaired electrons are 4.90 μ_B and 5.92 μ_B, respectively.[55] [b] References 50−52. [c] Reference 95. [d] Reference 53. [e] Reference 19. [f] The predicted μ_{eff} in D_2O. [g] The average difference.

(b) Sodium Dithionite. Sodium dithionite was found to reduce both {Mn^{III}BVDME}$_2$ and BVDME^{3-} into bilirubin. The experiments were done both in 9/1 methanol/aqueous solution (pH* 7.9) and in 1/1 methanol/0.05 M Tris buffer (pH 7.8) at 25 °C. The sodium dithionite to 1/2{Mn^{III}BVDME}$_2$ ratios were 40:1 and 750:1 with [{Mn^{III}BVDME}$_2$]$_{tot}$ = 6 μM (Figure 5B). The rate of the reduction was about 5-fold faster in 9/1 than in 1/1 MeOH/aqueous solutions.

(c) Reducing Radicals. {Mn^{III}BVDME}$_2$ was also reduced by the solvated electrons and hydroxymethyl radicals produced upon γ-irradiation in deoxygenated aqueous methanol (1/1) solutions at pH 7.0 (phosphate buffered) and pH 10.2. The spectral changes observed following irradiation with increasing doses were similar to those obtained with dithionite and indicated stepwise reduction into the demetalated BVDME^{3-}.

Reaction with Oxidants. Oxidation of 7 μM 1/2{Mn^{III}-BVDME}$_2$ was achieved with 1.3 × 10^{-4} M *m*-chloroperoxybenzoic acid in the presence and absence of 1.7 × 10^{-4} M $NaNO_2$ in 9/1 methanol/aqueous solution (pH* 7.9), and in 1/1 (v/v) methanol/0.05 M Tris buffer, as described[47−49] for the oxidation of Mn^{III}TM-4-PyP^{5+}. The same spectral changes were observed both with and without $NaNO_2$, and the former are shown in Figure 6. The oxidation is observed as an initial increase and subsequent decrease in the absorbance at 681 nm, followed by an increase in the 555 nm peak. Biliverdin dimethyl ester and bilirubin dimethyl ester were studied under the same conditions. No observable changes in the UV/vis spectrum of biliverdin dimethyl ester took place within 12 h. However, the spectrum of the reduced ligand, bilirubin dimethyl ester, underwent slow changes within the same time period, and the product was not biliverdin dimethyl ester. {Mn^{III}BVDME}$_2$ was also oxidized by the trichloromethylperoxyl radicals produced upon irradiation in aerated methanol solutions containing CCl_4. The spectral changes show a decrease of absorbance at all the peaks and formation of new bands at 552, 620, and 675 nm, similar to those in Figure 6.

Magnetic Susceptibility in Solution. The ^{1}H NMR spectra were obtained independently for both ligands and their man-

(46) Spasojević, I.; Batinić-Haberle, I. Unpublished results.
(47) Groves, J. T.; Lee, J.; Marla, S. S. *J. Am. Chem. Soc.* **1997**, *119*, 6269.
(48) Groves, J. T.; Stern, M. K. *J. Am. Chem. Soc.* **1987**, *109*, 3812.
(49) Czernuszewicz, R. S.; Su, Y. O.; Stern, M. K.; Macor, K. A.; Kim, D.; Groves, J. T.; Spiro, T. G. *J. Am. Chem. Soc.* **1988**, *110*, 4158.

Table 4. Comparison of Electrochemical Data and SOD Activities of $\{Mn^{III}BVDME\}_2$, $\{Mn^{III}BV^{2-}\}_2$, $Mn^{III}TM\text{-}2\text{-}PyP^{5+}$,[a] $Mn^{III}TE\text{-}2\text{-}PyP^{5+}$,[a] $Mn^{III}salen^{+}$, and Mn^{2+}

compound	$E_{1/2}$, V vs NHE[b] ($E_{1/2}$, V vs Ag/AgCl)	IC_{50}, M[c]	k_{cat}, M^{-1} s^{-1}	
			cyt c[c]	pr[d]
$Mn^{III/II}TM\text{-}2\text{-}PyP^{5+/4+}$	$+0.22^a(+0.12)^e$	4.3×10^{-8} [a]	6.0×10^{7}[a]	
$Mn^{III/II}TE\text{-}2\text{-}PyP^{5+/4+}$	$+0.23^a(+0.13)^e$	4.5×10^{-8} [a]	5.8×10^{7} [a]	5.4×10^{7}
$^1/_2\{Mn^{III/IV}BVDME^{0/+}\}_2$	$+0.45^f(+0.36)^e$	5.0×10^{-8}	5.0×10^{7}	$\sim 9 \times 10^{6}$
$^1/_2\{Mn^{III}BVDME\}_2/Mn^{II}HBVDME$	$-0.23^f(-0.32)^e$			
$^1/_2\{Mn^{III/IV}BV^{2-/-}\}_2$[g]	$+0.50^h(+0.25)^h$	5.0×10^{-8}	2.5×10^{7}	9.0×10^{6}
$Mn^{III/II}salen^{+/0}$	$-0.13^f(-0.23)^e$	1.3×10^{-6} [i]	6.0×10^{5} [i]	
Mn^{2+}			1.3×10^{6} [j]	1.9×10^{6} [j]

[a] Reference 3. [b] In aqueous solution, 0.05 M phosphate buffer, pH 7.8, 0.1 M NaCl. [c] Data obtained by the cytochrome *c* assay; standard uncertainties are estimated to be ±20%. IC_{50} is the concentration that causes 50% inhibition of the reduction of 10 μM cytochrome *c* by $O_2^{\bullet-}$, produced at a rate of 1.2 μM/min in 0.05 M phosphate buffer, pH 7.8 at (25 ± 1) °C. IC_{50} and k_{cat} are expressed per $^1/_2\{Mn^{III}BVDME\}_2$ and are determined with estimated standard uncertainties of ±20%. [d] Data obtained by pulse radiolysis in 0.05 M phosphate buffer, pH 7.8, 22 ± 1 °C; the standard uncertainties are ±30%. [e] In 9/1 (v/v) methanol/aqueous solution, pH* 7.9, V vs Ag/AgCl. [f] The extrapolated redox potential in aqueous solution. [g] The $^1/_2\{Mn^{III}BV^{2-}\}_2/Mn^{II}HBV^{2-}$ couple was poorly defined. [h] Data obtained in 0.05 M phosphate buffer, pH 7.8, 0.1 M NaCl. [i] No SOD-like activity was observed in the presence of EDTA. [j] Mn^{2+} in 0.05 M phosphate buffer, pH 7.8. All $E_{1/2}$ are determined with a standard uncertainty of ±3 mV.

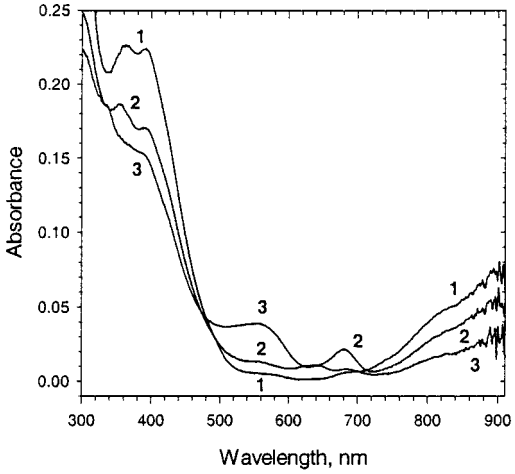

Figure 6. The oxidation of 7 μM 1/2$\{Mn^{III}BVDME\}_2$ with 0.13 mM *m*-chloroperoxybenzoic acid and 0.17 mM $NaNO_2$ in 9/1 (v/v) methanol/aqueous solution, pH* 7.9. Spectrum 1 was in the absence of oxidant, and spectrum 2 was 4 min and spectrum 3 was 1163 min after the addition of *m*-chloroperoxybenzoic acid and $NaNO_2$.

ganese complexes at 25 °C, permitting the measured susceptibilities to be corrected for the diamagnetic contribution of the ligand. The gram susceptibility, χ_g of the compound was calculated using eq 1

$$\chi_g = (3\Delta\nu)/(Q2\pi\nu_1 m) + \chi_o \quad (1)$$

where $Q = 2$ for the superconducting magnet, $\Delta\nu$ is the frequency difference in hertz between the shifted resonance and the t-BuOH reference peak from the inserted capillary insert tube, ν_1 is the frequency in hertz at which the proton resonances are studied, *m* is the mass in grams of the compound in 1 mL of the solvent, and χ_o is the mass susceptibility of the solvent, -0.72×10^{-6} cm^3 g^{-1} for D_2O and -0.66×10^{-6} cm^3 g^{-1} for CD_3OD.[42] The molar susceptibility, χ_M, was calculated as $\chi_M = \chi_g M$, where *M* is the molar mass. The effective magnetic moments, μ_{eff}, were then calculated from the eq 2 and are given in μ_B in Table 3:

$$\mu_{eff} = 2.84\sqrt{\chi_M T} \quad (2)$$

Since $\{Mn^{III}BVDME\}_2$ is methanol-soluble we measured its magnetic moment in CD_3OD and obtained a $\mu_{eff} = 4.57$ μ_B, which is lower than expected for a spin-only Mn(III) ion. We therefore performed susceptibility measurements both in deuterated water and methanol for several compounds of known metal oxidation states, but of different charge-to-hydrophilicity ratios. As control compounds of positive and negative charges we used $Mn^{III}TM(E)\text{-}2\text{-}PyP^{5+}$, $Mn^{III}TSPP^{3-}$, $Mn^{III}salen^{+}$ [18,50−52] and the Mn(II) complex $Mn^{II}OBTM\text{-}4\text{-}PyP^{4+}$.[5] The magnetic moments are given in Table 3. In all cases, independent of total charge, the μ_{eff} values of the standard compounds are lower in methanol than in water. On the basis of these differences we predict $\mu_{eff} = 5.10$ μ_B for $\{Mn^{III}BVDME\}_2$ in water, which is indicative of Mn(III). The same oxidation state was previously suggested for a similar compound, manganese(III) octaethylbilindione, based on a $\mu_{eff} = 4.7$ μ_B measured in chloroform.[53]

Magnetic Susceptibility in the Solid State. The measured gram susceptibilities (χ_g) of $\{Mn^{III}BVDME\}_2$ in the solid state were independent of the magnetic field strength from 300 to 3000 Oe at both 77 and 286 K, indicating the absence of the ferromagnetic impurities in the compound. Sixty χ_g values were obtained from 77 to 286 K, and Figure 7 shows the linear relationship between χ_g and $1/(T + 27.1)$, in accord with the Curie−Weiss law (eq 3)

$$\chi_g = \chi_d + C/(T - \Theta) \quad (3)$$

The Weiss constant Θ was equal to −27.1, and the Curie constant $C = (3.73 \pm 0.03) \times 10^{-3}$ emu/g/K. The diamagnetic gram susceptibility, χ_d, obtained from the intercept was $(-1.18 \pm 1.44) \times 10^{-7}$ emu/g. From eq 4,

$$C = N\mu^2\beta^2/3k \quad (4)$$

where *N* is the number of manganese ions/g, β the unit Bohr magneton, and *k* Boltzmann constant, the magnetic moment, μ, was calculated to be 4.45 μ_B (Table 3). Most coordination compounds show small positive or negative Weiss constants, and unless it is known that the compound is purely antiferromagnetic, the constant has little physical significance.[54] The inset in Figure 7 shows the decrease in the effective magnetic moment, μ_{eff}, as the temperature decreases, indicating antifer-

(50) Prabhakaran, C. P.; Patel, C. C. *J. Inorg. Nucl. Chem.* **1969**, *31*, 3316.
(51) Yarino, T.; Matsushita, T.; Masuda, I.; Shinra, K. *J. Chem. Soc. Chem. Commun.* **1970**, 1317.
(52) Prabhakaran, C. P.; Patel, C. C. *J. Inorg. Nucl. Chem.* **1968**, *30*, 867.
(53) Balch, A. L.; Mazzanti, M.; Noll, B. C.; Olmstead, M. M. *J. Am. Chem. Soc.* **1994**, *116*, 9114.
(54) Figgis, B. N.; Lewis, J. In *Modern Coordination Chemistry*; Lewis, J., Wilkins R. J., Eds.; Interscience: New York, 1960; p 400.

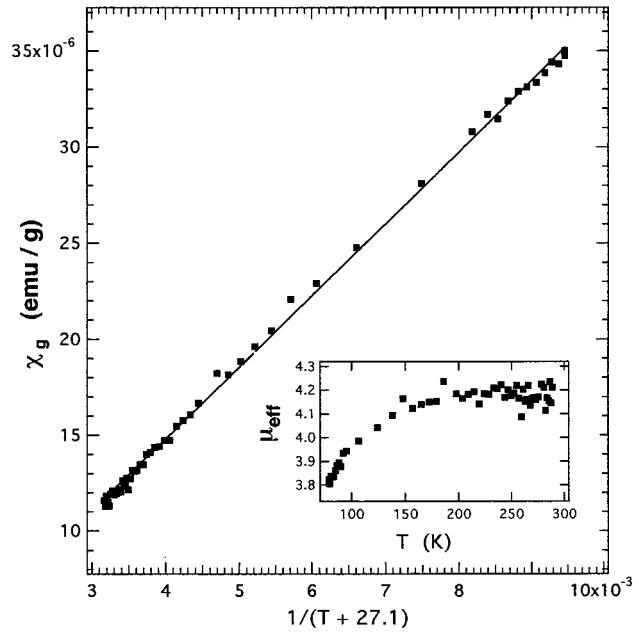

Figure 7. Magnetic susceptibility measurements of the solid $\{Mn^{III}BVDME\}_2$. The linear relationship between χ_g and $1/(T + 27.1)$ is in accord with Curie−Weiss law (eq 3). Inset: The decrease in μ_{eff} with a decrease in T.

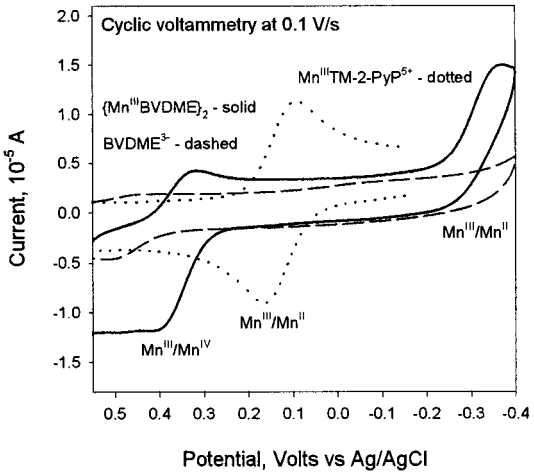

Figure 8. Cyclic voltammogram of $\{Mn^{III}BVDME\}_2$ and $BVDME^{3-}$ in 9/1 (v/v) MeOH/H_2O solution, pH* 7.9 (0.1 M NaCl), scan rate 0.1 V/s.

romagnetic "type" of behavior. The μ_{eff} at 298 K of ~4.25 μ_B or the μ of 4.45 μ_B are low compared to the spin-only value of 4.90 μ_B expected for high-spin Mn^{3+}. This could be a reflection of at least some spin−spin interactions in the solid state.

Electrochemistry. At a 0.1 V/s scan rate and in the +0.6 to −0.4 V region, the cyclic voltammetry of $\{Mn^{III}BVDME\}_2$ as compared to metal-free ligand $BVDME^{3-}$ reveals two new waves, one reversible and the other one irreversible (Figure 8). The irreversible wave at more negative potentials becomes reversible at higher scan rates (see below). The magnetic moment μ_{eff} = 5.10 μ_B, shown in Table 3, established +3[55] rather than +2 as a stable oxidation state of manganese in $\{Mn^{III}BVDME\}_2$. Further, the chronocoulometric measurements at constant potential confirmed +3 as the resting state of manganese in $\{Mn^{III}BVDME\}_2$ (Figure 9). No redox process was detected at +100 mV vs Ag/AgCl (between the two metal-

(55) Drago, R. S. *Physical Methods for Chemists*, 2nd ed.; Saunders College Publishing: Ft. Worth, 1977.

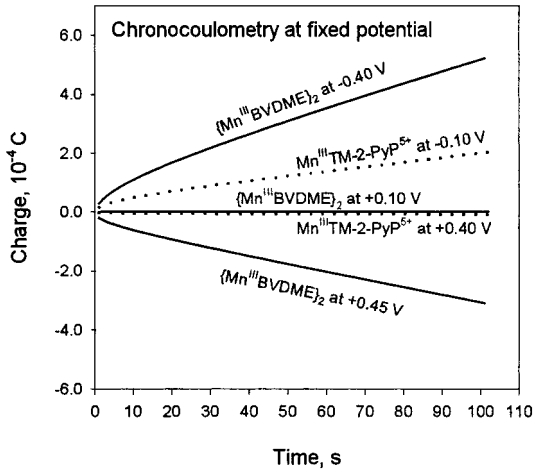

Figure 9. Fixed potential chronocoulometric measurements of 1 mM $1/2\{Mn^{III}BVDME\}_2$ and $Mn^{III}TM\text{-}2\text{-}PyP^{5+}$ in 9/1 (v/v) MeOH/H_2O, pH* 7.9 (0.1 M NaCl).

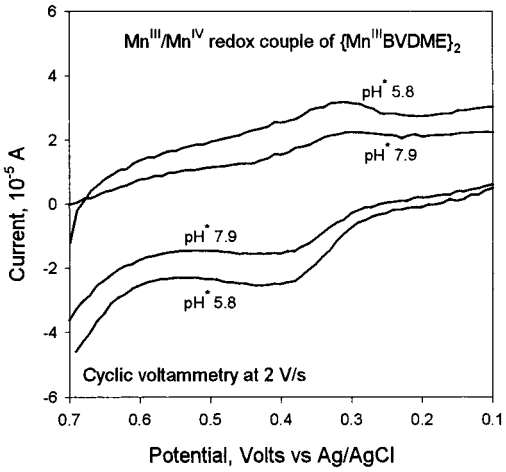

Figure 10. Cyclic voltammogram of 0.5 mM $1/2\{Mn^{III}BVDME\}_2$ in 9/1 (v/v) MeOH/H_2O, pH* 5.8 and 7.9, scan rate 2 V/s (0.1 M NaCl).

centered waves) while *oxidation* takes place at potentials more positive than one wave (+0.45 V vs Ag/AgCl) and *reduction* takes place at potentials more negative than another wave (−0.40 V vs Ag/AgCl). For comparison we utilized an electrochemically well-characterized manganese porphyrin $Mn^{III}TM\text{-}2\text{-}PyP^{5+}$, which, as expected, was reduced at −0.10 V vs Ag/AgCl but exhibited no electrochemistry at +0.40 V vs Ag/AgCl (Figure 9). We therefore ascribe the voltammogram at +0.36 V vs Ag/AgCl to the Mn(III)/Mn(IV) couple and the voltammogram at −0.32 V vs Ag/AgCl to the Mn(III)/Mn(II) couple. The voltammograms obtained have a peak-to-peak separation of 59 mV or higher, which means that the redox processes at the two metal centers in the dimeric $\{Mn^{III}BVDME\}_2$ complex occur independently. The reversible Mn(III)/Mn(IV) couple was proton-independent (Figure 10) and can be described by eq 5:

$$^1/_2\{Mn^{III}BVDME^0\}_2 \leftrightarrow {}^1/_2\{Mn^{IV}BVDME^+\}_2 + e^- \quad (5)$$

The quasi-reversible Mn(III)/Mn(II) couple was proton-dependent (Figure 11)

$$^1/_2\{Mn^{III}BVDME^0\}_2 + H^+ + e^- \leftrightarrow Mn^{II}HBVDME^0 \quad (6)$$

The Nernst equation, applied to a one-proton (per metal center), one-electron redox reaction, predicts a change in the

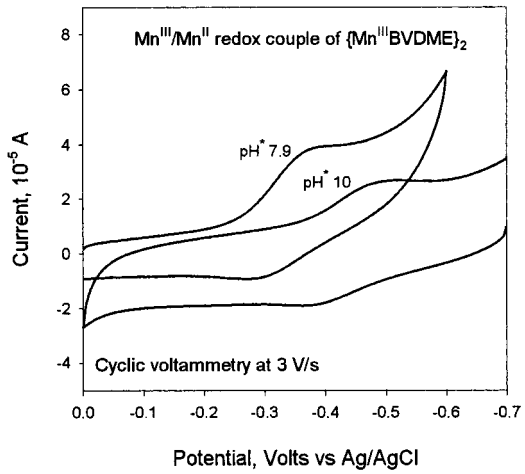

Figure 11. Cyclic voltammogram of 0.5 mM 1/2{Mn^{III}BVDME}$_2$ in 9/1 (v/v) MeOH/H_2O, pH* 7.9 and 10.0, scan rate 3 V/s (0.1 M NaCl).

redox potential of −59 mV per pH unit.[56] Accordingly, we observed a shift of −115 mV when the pH* was increased from 7.9 to 10.0. Once manganese is reduced to the +2 state, enolic oxygen binding is no longer favored and the dimeric structure either partially opens or falls apart accompanied by protonation of the enolic oxygen and eventual loss of the metal ion. Thus, electrochemical reversibility was only achieved at high scan rates (3−10 V/s), as shown in Figure 11.

Another support for the assignment of the observed voltammograms came from spectroelectrochemical measurements. The same spectral features, shown in Figure 12A, were obtained when a voltage of +500 mV was applied to the gold-mesh working electrode (3 mM 1/2{Mn^{III}BVDME}$_2$, 9/1 (v/v) methanol/aqueous solution, Tris buffer, pH* 7.9) as those observed upon the oxidation of {Mn^{III}BVDME}$_2$ with *m*-chloroperoxybenzoic acid (Figure 6). Also, when a voltage of −500 mV was applied, the spectral features observed (Figure 12B) resemble the spectra obtained upon metal-centered reduction of {Mn^{III}BVDME}$_2$ (Figure 5A). However, the applied voltage of −500 mV did not enable ligand-centered reduction, which, being in accordance with the voltammogram of the biliverdin dimethyl ester shown in Figure 8, supports the assignment of the voltammogram at −0.32 V vs Ag/AgCl to the redox cycling of the metal center. The redox potentials of {Mn^{III}BVDME}$_2$ obtained in 9/1 methanol/aqueous solutions as V vs Ag/AgCl were extrapolated to the $E_{1/2}$ in water and expressed in V vs NHE. The experimentally obtained and the extrapolated potentials are given in Table 4.

The cyclic voltammetry of {$Mn^{III}BV^{2-}$}$_2$ shows the same behavior discussed above for its dimethyl ester analogue, and the $E_{1/2}$ of the Mn(III)/Mn(IV) couple of both complexes were found at similar potentials (Table 4). Only a poorly defined wave for Mn(III)/Mn(II) was observed for {$Mn^{III}BV^{2-}$}$_2$.

Catalysis of $O_2^{\bullet-}$ Dismutation: **Cytochrome *c* Assay**. The rate constants for the reaction of the Mn complexes with $O_2^{\bullet-}$ were determined by competition kinetics using cytochrome *c* as the reference.[57] Possible interference with the xanthine/xanthine oxidase reaction by the test compounds was examined by following the rate of urate accumulation at 295 nm in the absence of cytochrome *c*. Mn(III) complexes did not interfere with reaction of xanthine with xanthine oxidase and did not directly interact with cytochrome *c* in the absence of $O_2^{\bullet-}$. The

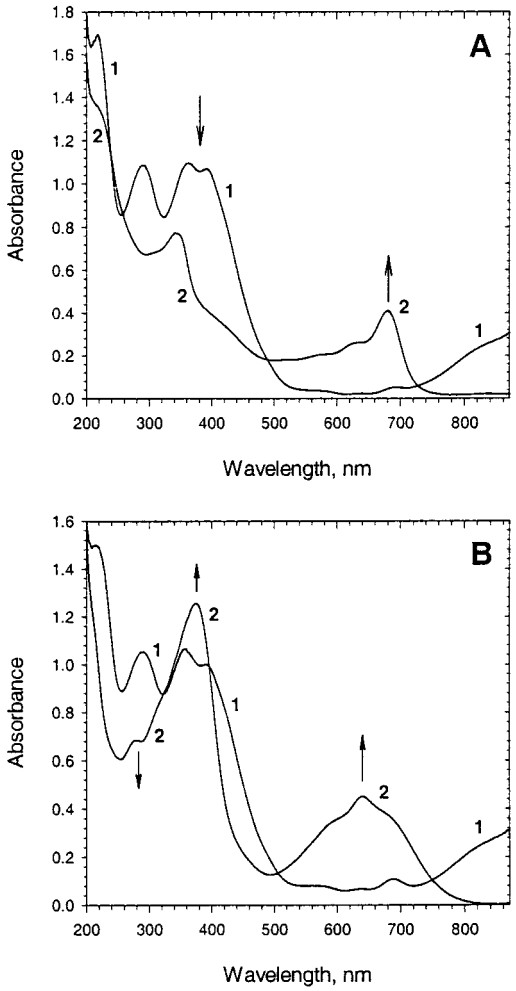

Figure 12. Spectroelectrochemistry of 3 mM 1/2{Mn^{III}BVDME}$_2$ in 9/1 (v/v) MeOH/H_2O, pH* 7.9, at an applied voltage of +500 mV within 9 min (A), and of −500 mV within 2 min (B).

reoxidation of cytochrome *c* by H_2O_2 (produced in xanthine/xanthine oxidase reaction) in the presence of Mn(II) complexes was observed and eliminated by the addition of catalase. Neither biliverdin nor bilirubin showed any observable SOD-like activity, consistent with the previous study of Robertson and Fridovich.[58] When added at 1:1 albumin-to-compound ratio, no negative effect of albumin was observed. At higher albumin-to-compound ratios the SOD-like activity decreases and is 50% lower when the ratio becomes 3:1. Typically, 10 μM stock methanolic solutions of 1/2{Mn^{III}BVDME}$_2$ were diluted to nanomolar levels in the aqueous assay solution. Inhibition of 10 μM cytochrome *c* reduction by the compound, when plotted as $\{(v_0/v_i) - 1\}$ vs $^1/_2$[{Mn^{III}BVDME}$_2$], yielded a straight line, as shown in Figure 13. The v_0 is the uninhibited rate of reduction of cytochrome *c* by $O_2^{\bullet-}$ and v_i the rate of cytochrome *c* reduction inhibited by the compound. From the plot, the concentration that causes 50% of the inhibition of cytochrome *c* reduction by $O_2^{\bullet-}$ (1 unit of activity) was found at $(v_0/v_i) - 1 = 1$, $IC_{50} = 4.7 \times 10^{-8}$ M. On the basis of the competition[57] with 10 μM cytochrome *c*, at 50% inhibition the rates of the reactions of cytochrome *c* and the mimic with $O_2^{\bullet-}$ are equal, i.e., $k_{cat}{}^1/_2$[{Mn^{III}BVDM}$_2$] = k_{cyt}[cytochrome *c*], where $k_{cyt} = 2.6 \times 10^5$ M^{-1} s^{-1}.[59] Hence, the catalytic rate constant was

(56) Astruc, D. *Electron Transfer and Radical Processes in Transition-Metal Chemistry*, pp 162, VCH Publishers: New York, 1995.
(57) Sawada, Y.; Yamazaki, I. *Biochim. Biophys. Acta* **1973**, *327*, 257.
(58) Robertson, P., Jr.; Fridovich, I. *Arch. Biochem. Biophys*. **1982**, *213*, 353.
(59) Butler, J.; Koppenol, W. H.; Margoliash, E. *J. Biol. Chem*. **1982**, *257*, 10747.

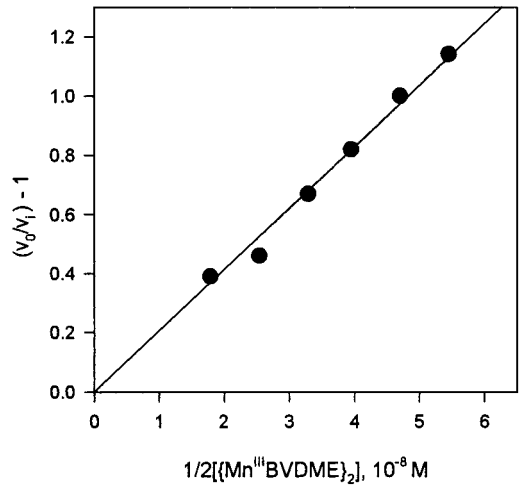

Figure 13. Plot of $\{(v_0/v_i) - 1\}$ vs $^1/_2[\{Mn^{III}BVDME\}_2]$. v_0 is the rate of reduction of 10 μM cytochrome *c* by $O_2^{\bullet-}$ and v_i the rate of reduction of cytochome *c* inhibited by the catalyst in the presence of 0.1 mM EDTA in 0.05 M Tris buffer at pH 7.8, 40 μM xanthine, ~ 2 nM xanthine oxidase at (25 ± 1) °C. The total volume of the assay solution is 3 mL.

calculated to be $k_{cat} = 5.0 \times 10^7$ M^{-1} s^{-1} at 25 °C (Table 4). The SOD-like activity of the water-soluble $\{Mn^{III}BV^{2-}\}_2$ was found to be similar to that of its dimethyl ester derivative (Table 4) and to that of Mn^{III}TM(E)-2-PyP^{5+}.[3,6] The catalytic rate constants determined by us[3−7] and others[2,60,61] employing the simple, straightforward, and widely used[62−64] indirect cytochrome *c* assay are identical to those determined for the same cationic manganese(III) *N*-alkylpyridylporphyrins by direct methods, such as pulse radiolysis[65,66] and the stopped-flow technique.[2,11,12,67] In addition to the cytochrome *c* assay we employed pulse radiolysis to study the catalytic properties of $\{Mn^{III}BV^{2-}\}_2$ and $\{Mn^{III}BVDME\}_2$.

The catalytic SOD-like behavior of Mn^{III}salen$^+$ was also studied by the cytochrome *c* assay and was observed only in the absence of EDTA.[68] In the presence of EDTA, the metal-centered reduction was accompanied by the loss of manganese.

Pulse Radiolysis. This technique permits direct spectrophotometric monitoring of the decay of $O_2^{\bullet-}$ radicals over the millisecond or shorter time scale and has been used to determine k_{cat} for a number of metal complexes.[65,66,69−71] The preferred method to produce $O_2^{\bullet-}$ radicals by pulse radiolysis is to use aqueous solutions of formate, where O_2 is reduced by the solvated electrons and by the $CO_2^{\bullet-}$ radicals from formate. However, since $\{Mn^{III}BVDME\}_2$ is not soluble in water in the micromolar range, we used aqueous methanol solutions instead. The $\bullet CH_2OH$ radicals, formed by the reactions of methanol with the H$^\bullet$ and $^\bullet$OH radicals in irradiated solutions, react with O_2 to form peroxyl radicals, $^\bullet O_2CH_2OH$.

$$H_2O \rightarrow e_{aq-}, H^\bullet, {}^\bullet OH, H^+, H_2, H_2O_2 \quad (7)$$

$$H^\bullet/{}^\bullet OH + CH_3OH \rightarrow H_2/H_2O + {}^\bullet CH_2OH \quad (8)$$

$${}^\bullet CH_2OH + O_2 \rightarrow {}^\bullet O_2CH_2OH \quad (9)$$

These radicals undergo elimination of $O_2^{\bullet-}$ in a base-catalyzed process,[72] e.g. with hydrogenphosphate ions.

$${}^\bullet O_2CH_2OH + HPO_4^{2-} \rightarrow O_2^{\bullet-} + CH_2O + H_2PO_4^- \quad (10)$$

To achieve rapid formation of $O_2^{\bullet-}$, we used 0.05 M phosphate buffer at pH 7.8 and found that reaction 10 is completed within several microseconds.

γ-Radiolysis of $\{Mn^{III}BVDME\}_2$ under such conditions did not yield any observable change in its UV/vis spectrum, even after producing a 20-fold excess of $O_2^{\bullet-}$ radicals over $\{Mn^{III}BVDME\}_2$, suggesting a catalytic function for the compound. Pulse radiolysis experiments were performed with 1/1 and 1/4 MeOH/aqueous (v/v) solutions of $\{Mn^{III}BVDME\}_2$. The initial concentration of $O_2^{\bullet-}$ produced by the pulse was 27 μM, and the concentration of $^1/_2\{Mn^{III}BVDME\}_2$ was varied between 1.5 and 10 μM. The dismutation of $O_2^{\bullet-}$ was followed at 280 nm. The rate constant was determined from the linear dependence of k_{obs} upon the concentrations of the catalyst. In 1/1 methanol/aqueous solution the rate constant obtained was $k_{cat} = (1.0 \pm 0.3) \times 10^6$ M^{-1} s^{-1}, while in 1/4 MeOH/aqueous solution $k_{cat} = (1.9 \pm 0.5) \times 10^6$ M^{-1} s^{-1}. A dependence of rate constant upon the methanol-to-water ratio was observed before.[73−75] A significant solvent effect was also observed in the reduction of $\{Mn^{III}BVDME\}_2$ by dithionite (see above). Due to the water-insolubility of $\{Mn^{III}BVDME\}_2$, k_{cat} could not be determined at lower methanol concentrations. Therefore, no good approximation to the conditions of cytochrome *c* assay (an all aqueous medium) could be achieved. Using the data obtained by Bielski et al.,[73,74] where the rate constant for the reaction of $O_2^{\bullet-}$ with cytochrome *c* in 35% ethanol was 4.3-fold lower than in the water, the rate constant in an all-aqueous medium may be considerably higher than the above values and closer to the value determined by the cytochrome *c* method.

The UV/vis and electrochemical characterization (Table 4) indicate that the water-soluble analogue, $\{Mn^{III}BV^{2-}\}$, is of the same nature as the dimethyl ester derivative. We, therefore, performed pulse radiolysis measurements with $\{Mn^{III}BV^{2-}\}_2$ in 0.05 M phosphate buffer, pH 7.8. The $\{Mn^{III}BV^{2-}\}_2$ is fairly stable for 30 min, which is sufficient time for the pulse radiolysis experiments. The rate constant determined from the plot of k_{obs} vs $^1/_2[\{Mn^{III}BV^{2-}\}_2]$ (Figure 14) is $k_{cat} = (9 \pm 3) \times 10^6$ M^{-1} s^{-1}. If we assume that a similar value is valid for $\{Mn^{III}BVDME\}_2$, this value is 5-fold lower than the rate constant determined by the cytochrome *c* assay. To directly compare the results obtained by the two methods, we performed pulse radiolysis measurements with Mn^{III}TE-2-PyP^{5+} and Mn(II)

(60) Pasternack, R. F.; Halliwell, B. *J. Am. Chem. Soc*. **1979**, *101*, 1026.
(61) Pasternack, R. F.; Skowronek, W. R., Jr. *J. Inorg. Biochem*. **1979**, *11*, 261.
(62) Yamakura, F.; Kobayashi, K.; Ue, H.; Konno, M. *Eur. J. Biochem*. **1995**, *227*, 700.
(63) Renault, J. P.; Verchere-Beaur, C.; Morgenstern-Badarau, I.; Yamakura, F.; Gerloch, M. *Inorg. Chem*. **2000**, *39*, 2666.
(64) Ohtsu, H.; Shimazaki, Y.; Odani, A.; Yamauchi, O.; Mori, W.; Itoh, S.; Fukuzumi, S. *J. Am. Chem. Soc.* **2000**, *122*, 5733.
(65) Faraggi, M. In *Oxygen Radicals in Chemistry and Biology*; Bors, W., Saran, M., Tait, D., Eds.; Walter de Gruyter: Berlin, Germany, 1984; p 419.
(66) Klug, D.; Rabani, J.; Fridovich, I. *J. Biol. Chem*. **1972**, *247*, 4839.
(67) Riley, D. P.; Rivers, W. J.; Weiss, R. H. *Anal. Biochem*. **1991**, *196*, 344.
(68) Liu, Z.-X.; Robinson, G. B.; Gregory, E. M. *Arch. Biochem. Biophys.* **1994**, *315*, 74.
(69) Weinraub, D.; Peretz, P.; Faraggi, M. *J Phys. Chem*. **1982**, *86*, 1839.
(70) Faraggi, M.; Peretz, P.; Weinraub, D. *Int. J. Radiat. Biol*. **1986**, *49*, 951.
(71) Solomon, D.; Peretz, P.; Faraggi, M. *J. Phys. Chem*. **1982**, *86*, 1842.
(72) Rabani, J.; Klug-Roth, D.; Henglein, A. *J. Phys. Chem.* **1974**, *78*, 2089.
(73) Bielski, B. H. J.; Gebicki, J. M. *J. Am. Chem. Soc*. **1982**, *104*, 796.
(74) Bielski, B. H. J. *J. Photochem. Photobiol*. **1978**, *28*, 645.
(75) Neta, P.; Huie, R. E.; Maruthamuthu, P.; Steenken, S. *J. Phys. Chem.* **1989**, *93*, 7654.

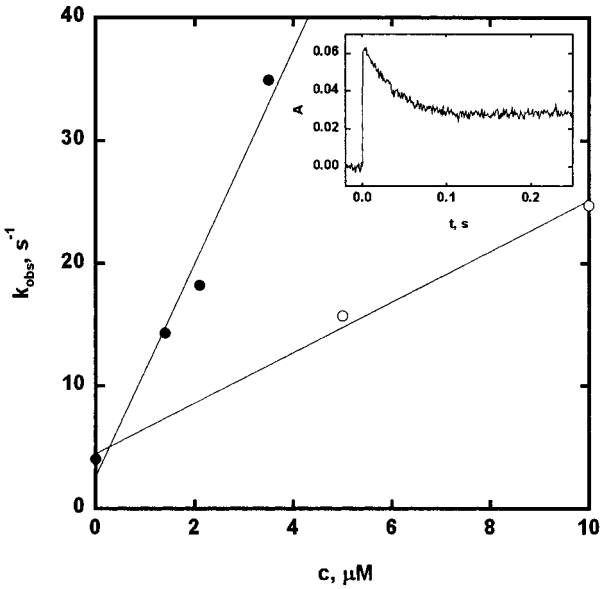

Figure 14. The dependence of the observed pseudo-first-order rate constant of the decay of $O_2^{\bullet-}$ radicals on the concentration of $^1/_2\{Mn^{III}BV^{2-}\}_2$ (solid circles) and Mn^{2+} (open circles) determined by pulse radiolysis in 0.05 M phosphate buffer, pH 7.8, at (22 ± 1) °C. The initial concentration of $O_2^{\bullet-}$ after the pulse was 27 μM. Inset: A kinetic trace showing the decay of $O_2^{\bullet-}$ at 280 nm.

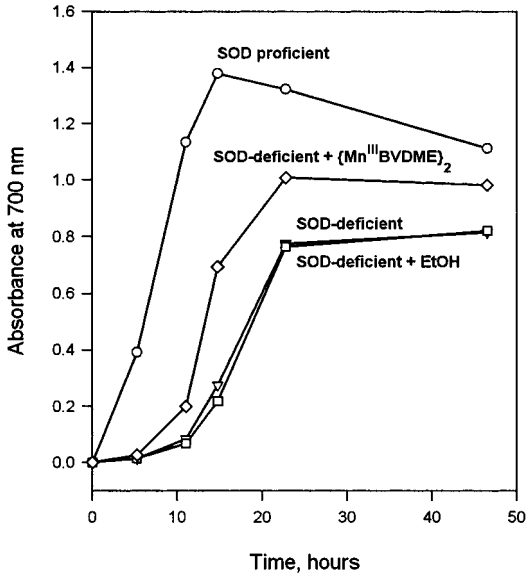

Figure 15. Growth curves of SOD-proficient AB1157 (circles) and SOD-deficient *E. coli* JI132 in the presence (13 μM) (diamonds) and absence of $\{Mn^{III}BVDME\}_2$ (triangle down) in minimal medium (five amino acids) under aerobic conditions, pH 7.8, 37 °C. The 20 mM ethanolic/albumin solution of compound was diluted into the medium. Also, the growth of SOD-deficient *E. coli* was followed in the presence of 0.15% ethanol only (squares).

phosphate[76] under the same conditions. The rate constants for $O_2^{\bullet-}$ dismutation by Mn^{III}TE-2-PyP^{5+} (Table 4)[76a] and by Mn^{2+}/phosphate buffer (Figure 14, Table 4)[76a,b] were found to be similar to those determined by the cytochrome *c* method. The catalytic rate constant for Mn^{2+} in phosphate buffer was $k_{cat} = 1.3 \times 10^6$ M^{-1} s^{-1} by the cytochrome *c* assay and $k_{cat} = (1.9 \pm 0.5) \times 10^6$ M^{-1} s^{-1} by pulse radiolysis (Table 4). We may presently attribute the differences in the rate constants of $\{Mn^{III}BV^{2-}\}_2$ and $\{Mn^{III}BVDME\}_2$ determined by the two methods to the difference in the concentration conditions applied, pulse radiolysis being performed at 2 orders of magnitude higher concentrations than the cytochrome *c* assay. The data may also imply, as suggested above by the ESMS data (Table 1), that at higher concentration levels a trimer exists in solution. Further studies with compounds of increased water solubility and increased metal/ligand stability are in progress.[76c]

Effects on *E coli*. When $\{Mn^{III}BVDME\}_2$ is added to the minimal medium at a concentration of 0.1−13 μM the growth of SOD-deficient *E. coli* was markedly improved. After 15 h, the SOD-proficient *E. coli* achieved 100% of its growth, and SOD-deficient achieved only 16% of its growth but 50% in the presence of 13 μM $\{Mn^{III}BVDME\}_2$ (Figure 15). The ligand $BVDME^{3-}$ itself was neither beneficial nor toxic and the Mn(III) complex did not affect the growth of the SOD-proficient *E. coli*.

Discussion

The biliverdin IXa formed by the oxidative attack of heme oxygenase[77−79] has been suggested to have antioxidant[80,81] and anti-HIV activity.[82] Also, a reduced form, bilirubin, was shown to protect neurons against oxidative stress injury.[83,84] We have examined the manganese complex of biliverdin to determine whether it or its parent ligand will exert antioxidant activity.

The stable complex, $\{Mn^{III}BVDME\}_2$, was formed in methanol from biliverdin dimethyl ester and a Mn(II) salt. The constant spectral properties over a wide range (10^{-8}−10^{-4} M) of concentrations suggest the presence of the same species. Electrospray mass spectrometry identified this species as the dimeric $\{Mn^{III}BVDME\}_2$ on the basis of major signals at *m*/*z* 1324 and 1325 at a cone voltage of 30 V. These peaks correspond to the oxidized and protonated dimer, respectively. The dimer persists both with an increase in the cone voltage from 30 to 180 V and with dilution. Increasing the cone voltage and the dilution increases the degree of the fragmentation, giving rise to the oxidized and protonated monomeric units at *m*/*z* 662 and 663. Freezing-point depression experiment gave unambiguous evidence that at 17 mM the compound is a dimer. This structural characterization is strongly supported by the X-ray structure of a similar model compound, the dimeric manganese(III) octaethylbilindione reported by Balch and co-workers.[53] Early investigations of manganese(III) and zinc(II) biliverdin dimethyl ester[19,20,85−88] suggested hydrogen bonding between the enolic proton and keto oxygen, giving a cyclic monomeric phlorin-type of structure. Although the +2 oxidation state of

(76) (a) Archibald, F. S.; Fridovich, I. *Arch. Biochem. Biophys.* **1982**, *214*, 452. (b) Batinić-Haberle, I.; Spasojević, I.; Neta, P.; Grodkowski, J.; Fridovich, I. unpublished results. (c) Batinić-Haberle, I.; Bommer, J. C.; Spasojević, I.; Neta, P.; Grodkowski, J.; Fridovich, I. Unpublished results.
(77) Sun, J.; Wilks, A.; Ortiz de Montellano, P. R.; Loehr, T. M. *Biochemistry* **1993**, *32*, 14151.
(78) Nakajima, O.; Gray, C. H. *Biochem. J.* **1967**, *104*, 20.
(79) Petryka, Z.; Nicholson, D. C.; Gray, C. H. *Nature* **1962**, *194*, 1047.
(80) Stocker, R.; Yamamoto, Y.; McDonagh, A. F.; Glazer, A. N.; Ames, B. N. *Science* **1987**, *235*, 1043.
(81) Nakagami, T.; Taji, S.; Takahashi, M.; Yamanishi, K. *Microbiol. Immunol*. **1992**, *36*, 381.
(82) Mori, H.; Otake, T.; Morimoto, M.; Ueba, N.; Kunita, N.; Nakagami, N.; Yamasaki, N., Taji, S. *Jpn. J. Cancer Res*. **1991**, *82*, 755.
(83) Dore, S.; Takahashi, M.; Ferris, C. D.; Hester, L. D.; Guastella, D.; Snyder, S. H. *Proc. Natl. Acad. Sci. U.S.A.* **1999**, *96*, 2445.
(84) Llesuy, S. F.; Tomaro, M. L. *Biochim. Biophys. Acta* **1994**, *1223*, 9.
(85) Wasser, P. K. W.; Fuhrhop, J.-H. *Ann. N. Y. Acad. Sci.* **1973**, *206*, 533.
(86) Fuhrhop, J.-H. *Angew. Chem., Internat. Ed*. **1974**, *13*, 321.
(87) Struckmeier, G.; Thewalt, U.; Fuhrhop, J.-H. *J. Am. Chem. Soc*. **1976**, *98*, 278.
(88) Koerner, R.; Olmstead, M. M.; Ozarowski, A.; Balch, A. L. *Inorg. Chem*. **1999**, *38*, 3262.

manganese was proposed,[19] the reported magnetic moment in chloroform of $\mu_{eff} = 5.15\ \mu_B$[19] would suggest a +3 rather than a +2 oxidation state for manganese.[55] Balch and co-workers have shown that Mn(III) and Fe(III) form dimers, while other metal ions such as Ni(II), Zn(II), Cu(II), and Co(II) exist as monomeric complexes.[53,89−94] Our magnetic moments in methanol and in the solid state, compared with those of known manganese compounds,[95,96] strongly support the +3 state in $\{Mn^{III}BVDME\}_2$[55] and are in agreement with measurements on the related manganese(III) octaethylbilindione in chloroform.[53]

The two redox systems of $\{Mn^{III}BVDME\}_2$ observed are assigned to metal-centered processes, since no electrochemistry of the biliverdin dimethyl ester was observed at such potentials. In addition, the spectral changes observed when a voltage of +500 mV was applied were identical as those observed upon oxidation with either *m*-chloroperoxybenzoic acid or with peroxyl radicals (Figure 12A). When a voltage of −500 mV (Figure 12B) was applied, the spectral changes observed were identical to those found upon reduction with either ascorbic acid or by γ-radiolysis. The metal-centered reduction is followed by dechelation to form biliverdin dimethyl ester and not the reduced form, bilirubin dimethyl ester. Since the resting oxidation state of the manganese center is Mn(III), we assign the voltammogram at $E_{1/2} = +0.36$ V vs Ag/AgCl to the Mn(III)/Mn(IV) couple and at $E_{1/2} = -0.32$ V vs Ag/AgCl to Mn(III)/Mn(II).

The relatively positive potential of the Mn(III)/Mn(IV) couple is favored by a dimeric structure that stabilizes Mn(IV) due to the binding of Mn(III) by the enolic oxygen atom (Scheme 1c,d). Thus the ligand is essentially trianionic in nature, as is the case with metallocorroles[97−101] or doubly N-confused porphyrins,[102] which also stabilize Mn(IV). The Mn^{III}TM-2(3,4)-PyP^{5+} compounds only form Mn(IV) at pH ≥ 11, where a Mn−OH (and not $Mn(OH_2)$) bond exists.[8]

We have previously established a structure−activity relationship[3] between the catalytic rate constants for the dismutation of the superoxide anion and the metal-centered reduction potentials for the water-soluble manganese(III) and iron(III) porphyrins. The closer the approach to the potential of superoxide dismutases ($E_{1/2} \sim +0.30$ V vs NHE)[103,104] or to the midpoint potential between the oxidation and reduction of $O_2^{\bullet-}$ ($E_{1/2} = +0.36$ V vs NHE),[105] the more potent the mimic.[3] The $E_{1/2}$ of Mn(III)/Mn(IV) and of Mn(III)/Mn(II) redox couples of $\{Mn^{III}BVDME\}_2$, extrapolated from methanol to water, are +0.45 V and −0.23 V vs NHE, respectively. A similar metal-centered redox potential for the Mn(III)/Mn(IV) couple was obtained for the $\{Mn^{III}BV^{2-}\}_2$ in water, $E_{1/2} = +0.50$ V vs NHE (Table 4). In Mn^{III}TM(E)-2-PyP^{5+}, the dismutation of $O_2^{\bullet-}$ is coupled to the Mn(III)/Mn(II) potential $E_{1/2} = +0.22(0.23)$ V vs NHE,[4] allowing these metalloporphyrin to be potent catalytic scavengers of $O_2^{\bullet-}$ with $k_{cat} = 6.0(5.8) \times 10^7\ M^{-1}\ s^{-1}$ (Table 4).[4] The Mn(III)/Mn(II) potential of $\{Mn^{III}BVDME\}_2$ is too negative to account for any efficient redox cycling of $O_2^{\bullet-}$.[3] Thus, it is the accessibility of the Mn(IV) state that enables $\{Mn^{III}BVDME\}_2$ to redox cycle $O_2^{\bullet-}$ (eqs 11 and 12) and to be a powerful mimic with $k_{cat} = 5.0 \times 10^7\ M^{-1}\ s^{-1}$, as determined by cytochrome *c* assay. As expected, on the basis of their similar $E_{1/2}$ values,[3] $\{Mn^{III}BV^{2-}\}_2$ and $\{Mn^{III}BVDME\}_2$ are similarly potent catalytic scavengers of $O_2^{\bullet-}$.

$$^1/_2\{Mn^{III}BVDME\}_2 + 2H^+ + O_2^{\bullet-} \leftrightarrow {}^1/_2\{Mn^{IV}BVDME^+\}_2 + H_2O_2 \quad (11)$$

$$^1/_2\{Mn^{IV}BVDME^+\}_2 + O_2^{\bullet-} \leftrightarrow {}^1/_2\{Mn^{III}BVDME\}_2 + O_2 \quad (12)$$

The cytochrome *c* assay and the pulse radiolysis were both used to determine k_{cat} for $\{Mn^{III}BVDME\}_2$, $\{Mn^{III}BV^{2-}\}_2$, Mn^{III}TE-2-PyP^{5+}, and manganese(II) phosphate (Table 4).[76a,b] The present and previously reported results[65,66] show that both methods, as well as the stopped-flow technique,[2,11,12,67] give the same kinetic results for manganese(III) *N*-alkylpyridylporphyrins and manganese(II) phosphate. While both the cytochrome *c* assay and the pulse radiolysis technique confirmed the catalytic nature of $\{Mn^{III}BVDME\}_2$ and $\{Mn^{III}BV^{2-}\}_2$, the rate constants obtained by pulse radiolysis were lower for both compounds. Work is in progress[76] to understand the cause of this discrepancy.

Groves and collaborators[11] previously showed that Mn^{III}TM-4-PyP^{5+} employs the Mn(III)/Mn(IV) couple while acting as an $O_2^{\bullet-}$-coupled peroxynitrite reductase. However, all the previously reported SOD mimics, whether Mn(III) (porphyrin[3−7,106,107] and salen complexes[18,108−110]) or Mn(II) compounds (pentaaza macrocyclic complexes,[2,111−115] Mn^{II}OBTM-

(89) (a) Attar, S.; Balch, A. L.; Van Calcar, P. M.; Winkler, K. *J. Am. Chem. Soc.* **1997**, *119*, 3317. (b) Attar, S.; Ozarowski, A.; Van Calcar, P. M.; Winkler, K.; Balch, A. L. *Chem. Commun*. **1997**, 1115.
(90) Balch, A. L.; Latos-Grazynski, L.; Noll, B. C.; Olmstead, M. M.; Safari, N. *J. Am. Chem. Soc.* **1993**, *115*, 9056.
(91) Balch, A. l.; Mazzanti, M.; Noll, B. C.; Olmstead, M. M. *J. Am. Chem. Soc*. **1993**, *115*, 12206.
(92) Bonfiglio, J. V.; Bonnett, R.; Buckley, D. G.; Hamzetash, D.; Hursthouse, M. B.; Abdul Malik, K. M.; McDonagh, A. F.; Trotter, J. *Tetrahedron* **1983**, *39*, 1865.
(93) Johnson, J. A.; Olmstead, M. M.; Balch, A. L. *Inorg. Chem*. **1999**, *38*, 5379.
(94) (a) Lord, P. A.; Olmstead, M. M.; Balch, A. L. *Inorg. Chem*. **2000**, *39*, 1128. (b) Balch, A. L. *Coord. Chem. Rev.* **2000**, *200−202*, 349.
(95) Hambright, P.; Turner, A.; Cohen, J. S.; Lyon, R. C.; Katz, A.; Neta, P.; Adeyemo, A. *Inorg. Chim. Acta* **1987**, *128*, L11.
(96) Boucher, L. J. *Coord. Chem. Rev*. **1972**, *7*, 289.
(97) Ghosh, A.; Wondimagegn, T.; Parusel, A. B. J. *J. Am. Chem. Soc*. **2000**, *122*, 5100.
(98) Gross, Z.; Galili, N.; Saltsman, I. *Angew. Chem., Int. Ed*. **1999**, *38*, 1427.
(99) Gross, Z.; Simkhovich, L.; Galili, N. *Chem. Commun*. **1999**, 599.
(100) Simkhovich, L.; Galili, N.; Saltsman, I.; Goldberg, I.; Gross, Z. *Inorg. Chem*. 2000, *39*, 2704.
(101) Mahammed, A.; Gross, Z. *Book of Abstracts;* First International Conference on Porphyrins and Phthalocyanines, Dijon, France, 2000, p 330.
(102) Furuta, H.; Maeda, H.; Osuka, A. *J. Am. Chem. Soc*. **2000**, *122*, 803.
(103) Lawrence, G. D.; Sawyer, D. T. *J. Am. Chem. Soc.* **1979**, *18*, 3045.
(104) Vance, C. K.; Miller, A.-F. *J. Am. Chem. Soc.* **1988**, *110*, 461.
(105) Wood, P. M. *Biochem. J*. **1988**, *253*, 287.
(106) Pasternack, R. F.; Banth, A.; Pasternack, J. M.; Johnson, C. S. *J. Inorg. Biochem*. **1981**, *15*, 261.
(107) Peretz, P.; Solomon, D.; Weinraub, D.; Faraggi, M. *Int. J. Radiat. Biol*. **1982**, *42*, 449.
(108) Baudry, M.; Etienne, S.; Bruce, A.; Palucki, M.; Jacobsen, E.; Malfroy, B. *Biochem. Biophys. Res. Commun.* **1993**, *192*, 964.
(109) Doctrow, S. R.; Huffman, K.; Marcus, C. B.; Malfroy, B. *Adv. Pharmacol.* 1997, *38*, 247.
(110) (a) Melov, S.; Ravenscroft, J.; Malik, S.; Gill, M. S.; Walker, D. W.; Clayton, P. E.; Wallace, D. C.; Malfroy, B.; Doctrow, S. R.; Lithgow, G. J. *Science* 2000, *289*, 1567. (b) Baker, K.; Marcus, C. B.; Huffman, K. Krut, H.; Malfroy, B.; Doctrow, S. R. *J. Pharmacol. Exp. Ther*. **1998**, *284*, 215.
(111) Salvemini, D.; Wang, Z.-Q.; Zweier, J. L.; Samouilov, A.; Macarthur, H.; Misko, T. P.; Currie, M. G.; Cuzzocrea, S.; Sikorski, J. A.; Riley, D. P. *Science* **1999**, *286*, 304.
(112) Riley, D. P.; Lennon, P. J.; Neumann, W. L.; Weiss, R. H. *J. Am. Chem. Soc.* **1997**, *119*, 6522.
(113) Riley, D. P.; Henke, S. L.; Lennon, P. J.; Weiss, R. H.; Neumann, W. L.; Rivers, W. J., Jr.; Aston, K. W.; Sample, K. R.; Rahman, H.; Ling, C.-S.; Shieh, J.-J.; Busch, D. H.; Szulbinski, W. *Inorg. Chem.* **1996**, *35*, 5213.
(114) Riley, D. P.; Weiss, R. H. *J. Am. Chem. Soc*. **1994**, *116*, 387.

4-PyP^{4+},[5] and others[116]), catalytically scavenge $O_2^{\bullet-}$ by employing the Mn(III)/Mn(II) redox couple. {Mn^{III}BVDME}$_2$ and {Mn^{III}BV^{2-}}$_2$ are the first compounds that utilize the Mn(III)/Mn(IV) couple for $O_2^{\bullet-}$ dismutation.

An enolic oxygen occupies the fifth coordination site of the Mn in the dimer, and in principle $O_2^{\bullet-}$ could bind at the sixth position, leading to an inner-sphere electron transfer process. However, we tend to favor an outer-sphere mechanism for the dismutation, as suggested previously for the aquamanganese(III) and monohydroxoiron(III) porphyrins.[3] The lack of reactivity of {Mn^{III}BVDME}$_2$ toward NO$^{\bullet}$ increases its specificity toward $O_2^{\bullet-}$. The complex exhibits 4 orders of magnitude higher stability toward degradation by H_2O_2 than the similarly potent catalytic scavenger of $O_2^{\bullet-}$, Mn^{III}TM(E)-2-PyP^{5+}. The inertness of {Mn^{III}BVDME}$_2$ toward H_2O_2, combined with its lack of reactivity with NO$^{\bullet}$, provides a specificity for $O_2^{\bullet-}$ reminiscent of that of the SOD enzyme itself.

The in vivo studies presented in Figure 15 show a significant protection of the SOD-deficient *E. coli* in the presence of (Mn^{III}BVDME}$_2$. The *E. coli* model has been used as a simple reliable model for oxidative injury. Typically, the compounds that proved to be efficient in this model were also powerful in the rodent models of oxidative injuries.[10] The ligands biliverdin and bilirubin showed neither significant $O_2^{\bullet-}$- nor H_2O_2-related activity.

Acknowledgment. The authors are grateful to Aeolus/Incara and Duke Comprehensive Cancer Center, Grant P30 CA 14236, for financial support. P.H. and A.N.T. are grateful to the Howard University CSTEA project, NASA contract NCC 5-184, for support.

Abbreviations

{Mn^{III}BVDME}$_2$: manganese(III) biliverdin IX dimethyl ester dimer.

{Mn^{III}BV^{2-}}$_2$: manganese(III) biliverdin dimer.

H_4BV^+: biliverdin IX (+1 charge when all the propionic acid groups are undissociated).

H_4BR: bilirubin IX (neutral when all the propionic acid groups are undissociated).

{Mn^{III}OEB}$_2$: manganese(III) octaethylbilindione.

H_4BVDME^+: biliverdin IX dimethyl ester.

H_4BRDME: bilirubin IX dimethyl ester.

H_2salen: salen, *N*,*N*′-bis(salicylidene)ethylenediamine.

Mn^{III}salen$^+$: manganese(III) salen.

Mn^{III}OEP$^+$: manganese(III) 2,3,7,8,12,13,17,18-octaethylporphyrin.

Mn^{III}TCPP^{3-}: manganese(III) 5,10,15,20-tetrakis(4-carboxylatophenyl)porphyrin (carboxylates are deprotonated in this abbreviation).

Mn^{III}TSPP^{3-}: manganese(III) 5,10,15,20-tetrakis(4-sulfonatophenyl)porphyrin.

Mn^{III}TM(E)-2(3,4)-PyP^{5+}: manganese(III) 5,10,15,20-tetrakis(*N*-methyl(ethyl)pyridinium-2(3,4)-yl)porphyrin; 2-*ortho*, 3-*meta*, and 4-*para* isomer.

Mn^{II}OBTM-4-PyP^{4+}: manganese(II) 2,3,7,8,12,13,17,18-octabromo-5,10,15,20-tetrakis(*N*-methylpyridinium-4-yl)porphyrin.

PBS: phosphate-buffered saline.

NO$^{\bullet}$: nitric oxide.

SOD: superoxide dismutase.

pH*: an asterisk is used to indicate that the pH is referred to an infinitely diluted solution in 9/1 methanol/aqueous solvent system rather than to the infinitely diluted solution in water.[22]

μ_B: Bohr magneton.

AB1157: SOD-proficient, wild-type strain of *E. coli*.

JI132: SOD-deficient, sodAsodB strain of *E. coli*

IC0004986

(115) Riley, D. P. *Adv. Supramol. Chem.* **2000**, *6*, 217.
(116) Xiang, D. F.; Duan, C. Y.; Tan, X. S.; Hang, Q. W.; Tang, W. X. *J. Chem. Soc., Dalton Trans.* **1998**, 1201.